DESIGN, CONSTRUCTION AND ANALYSIS

OF

CEILING FAN CLEANING ROBOT

LEE MUN HOE

BACHELOR OF MECHATRONICS ENGINEERING

UNIVERSITI TEKNIKAL MALAYSIA MELAKA

“ I hereby declare that I have read through this report entitle “Design, Construction and Analysis of Ceiling Fan Cleaning Robot” and found that it has comply the partial fulfillment for awarding the degree of Bachelor of Mechatronics Engineering.

Signature :

Supervisor‟s Name : Dr. Fariz Bin Ali @ Ibrahim

Date :

DESIGN, CONSTRUCTION AND ANALYSIS

OF

CEILING FAN CLEANING ROBOT

LEE MUN HOE

A report submitted in partial fulfillment of the requirements for the degree of Bachelor of Mechatronics Engineering

Faculty of Electrical Engineering

UNIVERSITI TEKNIKAL MALAYSIA MELAKA

2014 / 2015

I declare that this report entitle “Design, Construction and Analysis of Ceiling Fan Cleaning Robot” is the result of my own research except as cited in the references. The report has not been accepted for any degree and is not concurrently submitted in candidature of any other degree.

Signature :

Name : Lee Mun Hoe

Date :

ACKNOWLEDGEMENT

For the preparation of this report, I would like to express my gratitude to everyone who supported me throughout the course of this final year project. In particular, I am thankful to my supervisor Dr. Fariz Bin Ali @ Ibrahim for his aspiring guidance, teaching and motivation during the project work. Dr. Fariz is a dedicated supervisor and he always concerned about my working progress and ensures the task I had done are fulfilling the requirement of this project.

Besides that, I would like to thank my fellow friends for their friendly advice during the project work. Their point of view and invaluably constructive criticism are the fundamental to the improvement of the project.

Lastly, I am sincerely grateful to everyone for sharing their truthful and illuminating views on a number of issues related to the project. They guide me in term of technical knowledge and supportive idea during the progressing of this project.

ABSTRACT

The traditional ways of cleaning the ceiling fan required users use a dry dust cloth and get up to the height of ceiling fan using a step ladder, or use an extension rod with a brush. However, these methods are dangerous because users may fall down from the ladder and cause environment hygiene problem. Hence, alternative solution has proposed by design a ceiling fan cleaning robot. Meanwhile, the problems that should take into consideration are the weight of robot, different size of the fan blade, and physical structure of the robot. Consequently, the objective of this project is to design and develop a ceiling fan cleaning robot and analyse the performance of it by considering robot locomotion. Furthermore, there are some important criteria in the methodology of this project. The body structure of fan cleaning robot is designed using SolidWorks software, and several technologies are combined to accomplish the basic features of the robot. This is included the material selection of mechanical parts, such as body structure and cleaning equipment; power supply for robot in electrical parts; and electronic components, like an Arduino Leonardo microcontroller, infrared sensors and limit switch, DC motors with gears as actuators, and also indicators like LEDs and buzzer. A series of experiments are conducted to analyse the performance of the robot, such as rotational speed of DC motor; sensitivity of infrared sensor; accuracy of digital compass. And also, experiment to determine the difference between rechargeable battery and power adapter on weight of robot, velocity, and swinging angle on fan blade. The experimental results confirm the proposed methodology; and showed that the power adapter is preferable as power supply for fan cleaning robot. In summary, the fan cleaning robot can be developed with future expansion in mind.

ABSTRAK

Kaedah tradisional untuk membersihkan kipas siling memerlukan pengguna menggunakan kain kering dan memenjat tangga sehingga ketinggian kipas siling atau menggunakan batang sambungan dengan berus. Walau bagaimanapun, kaedah tersebut adalah bahaya kerana pengguna berkemungkinan akan terjatuh dari tangga dan menyebabkan masalah kebersihan alam sekitar. Oleh itu, penyelesaian alternatif telah dicadangkan dengan mereka bentuk robot pembersihan kipas siling. Sementara itu, masalah yang perlu diambil kira adalah berat robot, perbezaan saiz bilah kipas, dan struktur fizikal robot. Oleh yang demikian, objektif projek ini adalah untuk mereka bentuk dan membina sebuah robot pembersihan kipas siling dan menganalisis prestasi sistem robot dari segi pergerakan robot. Tambahan pula, terdapat beberapa kriteria penting dalam metodologi projek ini. Struktur badan robot direka bentuk dengan menggunakan perisian SolidWorks, dan gabungan beberapa teknologi untuk mencapai ciri-ciri asas robot. Ini termasuklah pemilihan bahan bahagian mekanikal, seperti bahan untuk membina struktur badan robot dan peralatan pembersihan; bekalan kuasa dan komponen elektronik dari segi elektrik dan elektronik, seperti pengawal mikro, pengesan dan penunjuk. Beberapa eksperimen telah dilakukan untuk menganalisis prestasi robot, ini termasuklah kelajuan DC motor; kepekaan pengesan inframerah; ketepatan kompas digital. Selain itu, eksperimen untuk mengkaji perbezaan di antara bateri boleh dicas semula dan plag penyesuai pada berat robot, halaju dan sudut berayun pada bilah kipas. Hasilnya, eksperimen dapat mengesahkan kaedah metodologi yang dicadangkan; dan menunjukkan plag penyesuai adalah lebih baik sebagai bekalan kuasa untuk robot pembersihan kipas siling. Kesimpulannya, robot pembersihan kipas siling boleh dikaji dan dikembangkan pada masa depan.

TABLE OF CONTENT

CHAPTER TITLE PAGE

LIST OF TABLES

LIST OF FIGURES

LIST OF ABBREVIATIONS

DSP	-	Digital Signal Processor
MIPS	-	Million Instructions Per Second
CPR	-	Count per Revolution
EEPROM	-	Electrically Erasable Programmable Read-Only Memory
CPU	-	Central Processing Unit
A/D converter	-	Analog-to-digital converter
DIO channel	-	Digital input / output channel
LAN	-	Local Area Network
RC	-	Radio Control
V	-	Travelling velocity
$\dot{\theta}$	-	Angular velocity of robot attitude
ω_L , ω_R	-	Rotational velocity of left and right wheels
W	-	Tread
R	-	Radius of wheel
ζ_L , ζ_R	-	Output duty rate of PWM motor control
ζ_{L0} , ζ_{R0}	-	Initial velocity of robot travelling expressed as duty rate
K_P	-	Feedback gain
IR LED	-	Infrared Light Emitting Diode
α	-	Angle of inclination of the plane to the horizontal
W	-	Weight of the robot
h-r	-	Height of the centre of gravity above the axle plane
H	-	Height of incline plane
r	-	Distance between the centres of the wheels to incline plane
b	-	Perpendicular distance of centre of gravity from the rear axle
a	-	Perpendicular distance of centre of gravity from the front axle
L	-	Distance between the centres of the rear and front wheels
R_A	-	Total normal reaction between the ground and the front wheels
R_B	-	Total normal reaction between the ground and the rear wheels

LIST OF APPENDICES

CHAPTER 1

INTRODUCTION

1.1 Motivation

Industrial robotics researches have been around since a long time ago. They are widely used in industrial to increase the efficiency of the manufacturing process. However, these researches and technologies have been emerged with the development of service robots to perform service useful to the community regardless in semi- or fully autonomous, such as medical robots, underwater robots and other type of robot that can carry out a multitude of jobs [1]. Therefore, service robots have become more active than ever due to demand of people"s need and market grows.

One of the service robots of everyday tools for people is the home appliance cleaning robot, particularly a floor cleaning robot. Normally, these cleaning robots are integrated with vacuum pump and rotating brushes to sweep floors. Hence, these robots can help people perform cleaning task which is usually tedious and repetitive. One of the advantages of these residential cleaning robots is that it does not require any complex moving parts.

According to Science News, there are about 610,000 autonomous vacuum cleaners and lawn-mowers were in operation by the end of 2003 and this number is deemed to increase throughout the years [2]. Based on Figure 1.1, a tendency increasing of US patents in cleaning robot from 2000 to 2013. This is shown a reasonable prediction by Science News about the market grows of cleaning robot, although the numbers shown in 2013 is not the total number of patents published [1].

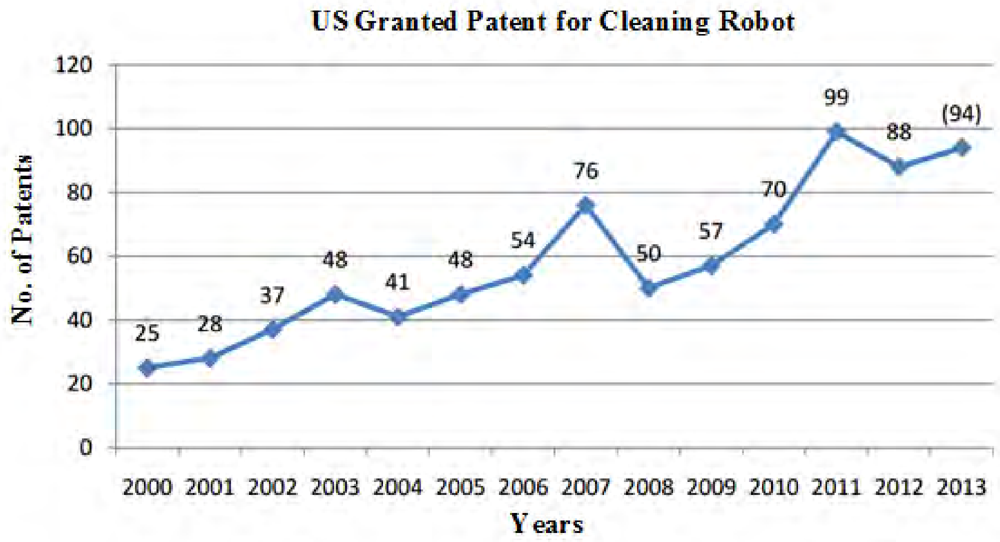

Figure 1.1: US granted patents from 2000 to 2013 [1].

Meanwhile, the developments of cleaning robot still a big gap to commercialize in the market, although some of the advanced robots have powerful functions, such as the navigation system and high efficiency of cleaning performance. Some of the possible reasons are the residential robot designed needed to consider the use for non-professional users, and the unreachable cleaning function of the robot in some area [1] like outside area of the building. These dangerous areas are needed to take further attention before developed to be marketed, especially think about the elder users.

On the other hand, according to French researchers, cleaners are suffering from exposure to many high risk factors for musculoskeletal disorders (MSDs). There are about 74% reported cleaners are experiencing muscular aches, and 52% of them sought for medical advice. About 46% experienced low back pain, 33% suffer neck and upper limb disorders, 22% to 24% is right wrist or hand, right shoulder and knee pain [3]. However, the occurrence of MSDs is mainly due to prolonged work with overhead cleaning. They have to do their jobs with a flexed or twisted body under long duration of cleaning tasks. Besides that, a study report claimed that 54% to 74% of all cleaners expose to continuous repetitive movement [3].

In consequence, ceiling fan is one of the unreachable places to be cleaned and overhead cleanest. It is common that dirt deposited on the surfaces of fan blades after the ceiling fan is used for a certain period. The traditional way to clean the ceiling fan is to wipe the dust from the blades. Users need to use a step ladder to get up to the height of fan blades and clean with a dry dust cloth, or a dust cloth coated with some cleaning solution. However, this can be dangerous for the person who does the cleaning task is at risk of falling down from the ladder [4].

On the other hand, an extension rod with brush is an alternative way can use for cleaning the ceiling fan, and reduce the risk of falling down from the ladder. But, the cleaning method is not effective as the surfaces of the blades are not fully cleaned and the dust from the blades will spread to surrounding, causing the environment hygiene problem. Hence, users need to sweep the dust on the floor after using the long stick with brush for cleaning the ceiling fan, however, this is spending and wasting of their time [5].

Thus, these factors have emerged to the interest in designing residential cleaning robot for different cleaning station and ceiling fan cleaning robot implementation would be the start of it.

1.2 Problem Statement

For the ceiling fan cleaning robot, the theoretical knowledge of static and dynamic mechanisms of a moving object is needed in designing and develops the robot. The fan cleaning robot needs to achieve stable moving motion on ceiling fan blades with appropriate speed. Therefore, actuator with higher torque is needed to actuate the robot and move on fan blade; and also it can stop instantly with minimum inertia and momentum to prevent it from falling down. This element is important in developing the robot structure.

Furthermore, the weight of the robot is needed to take into account. After the robot is placed on fan blade, the blade will be pushed downwards. Hence, the material chosen to build the robot is important, so that the robot won‟t damage to the ceiling fan, and can operate normally. Another aspect needed to be considered is the hardware component selection can influence the overall performance of the system. There are different designs of ceiling fan available in the market, particularly the fan blade designed by manufacturer to increase the airflow efficiency. Therefore, the development of fan cleaning robot is needed to consider the size of fan blade since it needs to move on it. A design of the flexible pulley in fan cleaning robot can be used to guide the robot move on the fan blade by pressing from both sides of the fan blade.

In addition, basic knowledge of the Arduino microcontroller using C language to design the control algorithms is needed. The algorithm loaded in the microcontroller is used to control the operation of the robot integrated with input and output electronic components. And also, the most important criteria for fan cleaning robot are the analysis of the robot locomotion mechanism to achieve the optimum performance of the robot.

1.3 Objectives

To complete this project, the following objectives are to be achieved at the end of this research:

1. To design and develop a semi-autonomous ceiling fan cleaning robot.
2. To analyse the system performance of the ceiling fan cleaning robot by considering robot locomotion.

1.4 Scopes

1. The fan cleaning robot is controlled by Arduino Leonardo as the main microcontroller to operate the robot system.
2. The robot is designed to move in forward and reverse direction only to remove the dust on the fan blades.
3. The body of the robot is constructed using plywood that is lightweight and cheap.
4. Infrared sensor and limit switch are integrated with the robot to detect the edge of fan blade to prevent from falling down.
5. Small pulleys are added to guide the robot moving in a straight line forward and reverse direction.
6. An extension rod is used to place the robot on the ceiling fan blade.
7. The dust cleaning analysis is not included in this report.

1.5 Report Outlines

This project focuses on the design and construction of the fan cleaning robot. The organization of this report is as follows:

1. Chapter 1 is to identify the development of cleaning robot and introduces the idea of ceiling fan cleaning robot. This chapter also covered the goals to be achieved and scope of this project.
2. Chapter 2 is the literature review of the previous work of researches about the cleaning robot.
3. Chapter 3 describes the methodology to design and construct the ceiling fan cleaning robot. This chapter also describes the method used to examine the performance of robot in terms of robot locomotion.
4. Chapter 4 discusses the findings obtained using statistical techniques and also the evaluation of the results.
5. Chapter 5 concludes the project findings and recommendation for future research.

CHAPTER 2

LITERATURE REVIEW

2.1 Design and Basic Construction

In order to develop a fully autonomous floor cleaning robot with the navigation system to avoid obstacles and perform the cleaning task efficiently, the LG‟s Roboking has been introduced by Core Technology Group, as shown in Figure 2.1 [6]. Roboking has a total number of 24 sensors to gather the environmental information for navigation purpose, included 14 ultrasonic sensors: 5 sensors to detect tall obstacles and 9 sensors to find flat obstacles. And also, 8 infrared sensors for cliff detection and to seek the charging station respectively, while another 2 tactile sensors for detecting small and slender objects [6].

Figure 2.1: Roboking [7].

Roboking has built in Texas instruments 320LF2406A digital signal processor (DSP) to control the robot operation, such as motor on board. This processor can run at 40 MHz with 40 MIPS (Million Instructions Per Second) performance [6].

In addition, a 12V / 3Ah nickel-metal hydride rechargeable battery is implemented on the robot as a power source. Once the battery power is low, Roboking can navigate itself back to the charging station automatically. Two types of DC motor have been used: a 12V, 70W suction power for suction nozzle work with rotating brushes as cleaning equipment, and 12V, 15W for navigation motor. The encoder is used for motor control which has 180 Count per Revolution (CPR) resolution [6]. Figure 2.2 is shown the Roboking system circuit block diagram.

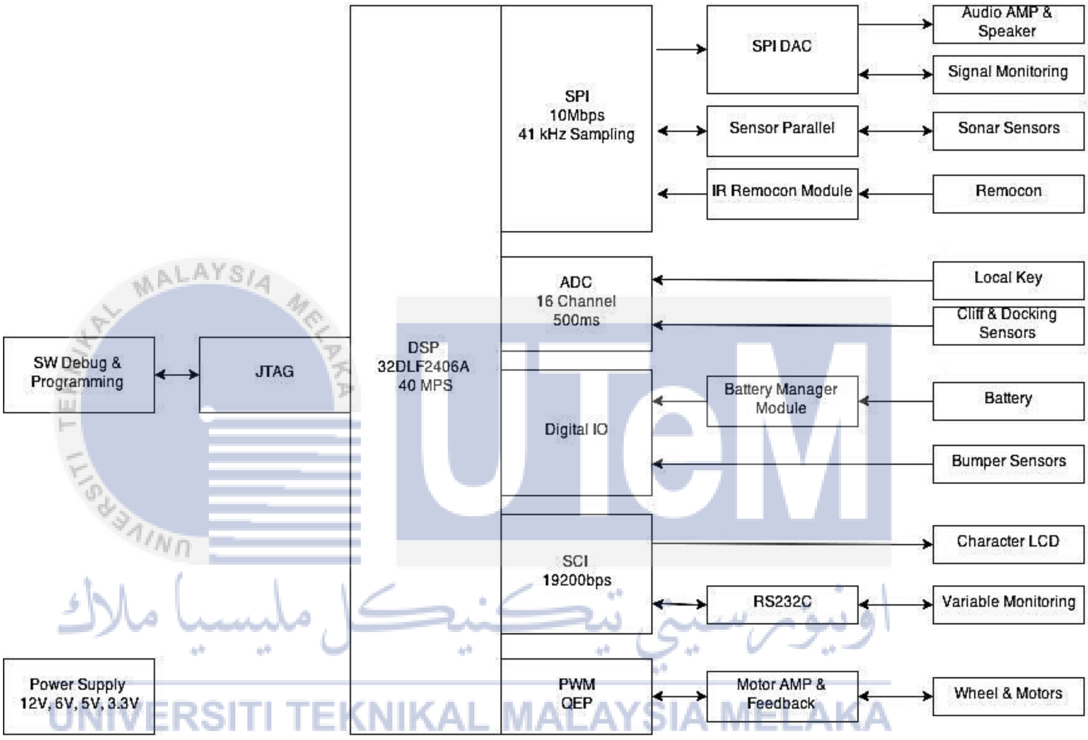

Figure 2.2: Roboking system circuit block diagram [6].

On the other hand, a floor cleaning mobile robot for domestic use has been proposed by Jordi. There are a few types of sensor built in this robot, including infrared sensors to prevent the robot from falling down stairs, mechanical contact sensors detect the obstacles, and Polaroid 6500 series ultrasonic sensors allowed the robot planning and building the path for mobility as well as wall alignment [8]. The cleaning device for this floor cleaning robot is an electric broom manufactured by Karcher. The roller brush is battery-powered, which can clean the floor using a friction mechanism and prevent dust generation by generating a suction airflow [8]. Figure 2.3 is shown the proposed cleaning robot by Jordi.

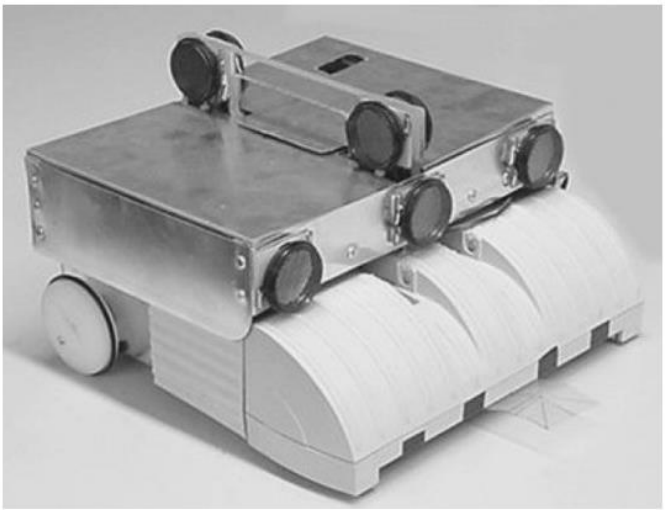

Figure 2.3: Cleaning robot proposed by Jordi [8].

Next, three microcontrollers have been used for robot control in Jordi"s floor cleaning robot. The main microcontroller has a memory bank of 256 KB built using I2C EEPROM devices, which enable the robot to store the environment map. [8] Then, a 6V lead-acid battery is used as power supply for the robot and rechargeable by using recharge equipment. Two DC geared Maxon motors are used for robot travelling and one brush motor for fixes cleaning intensity. A Hewlett Packard digital encoder with 1000 pulses per turn has built in the Maxon motor for speed measurement [8]. Figure 2.4 is shown the robot control diagram for the floor cleaning robot.

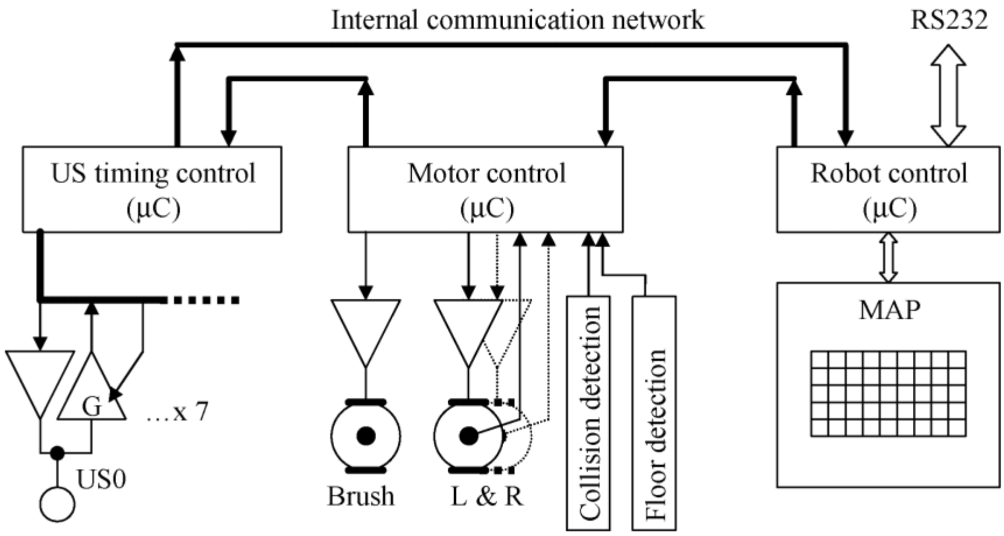

Figure 2.4: Floor cleaning robot control diagram [8].

In contrast, researchers had also fabricated a cleaning robot to perform cleaning tasks at the outside surface of the building, such as window glass of the modern architecture. A prototype of window cleaning robot shown in Figure 2.5 had been developed by Miraikikai Inc. The robot is small, lightweight and portable to perform the cleaning on a single large windowpane [9].

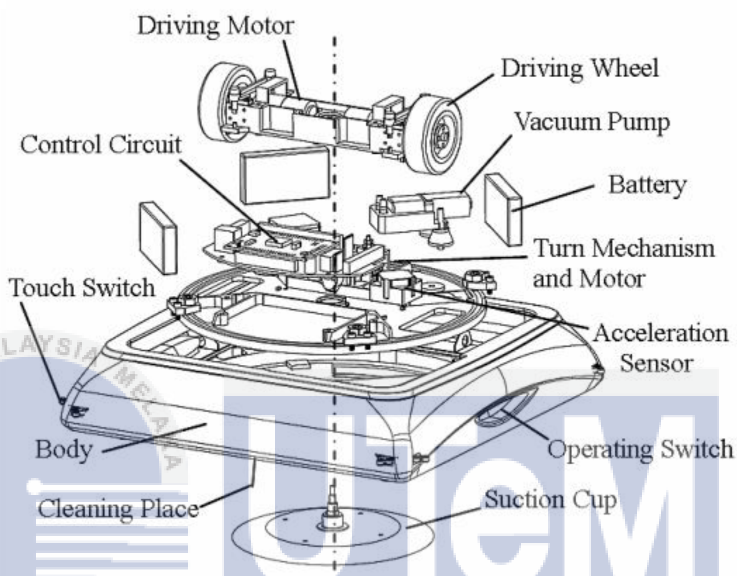

Figure 2.5: Mechanism of small-size window cleaning robot [9].

There are two types of sensors used on this window cleaning robot, which is touch switch and acceleration sensor The function of the touch switch is to detect the corner of windowpane while the robot travel from place to place, and the acceleration sensor is used for altitude control to detect the convoluted value between the acceleration of gravity and acceleration by the motion of the robot. A vacuum pump with maximum pressure 33.3 kPa and flow volume of 2.5 l/min is used as cleaning equipment to get rid of all the dust from the window surface [9].

Besides that, this window cleaning robot is implemented a PC 104 embedded controller to control the robot operation. This controller is a type of CPU Pentium 166 MHz, had built in with A/D converter, DIO channels, motion control and wireless LAN card. Next, the power supply for this robot is lithium-polymer battery with maximum current of 30 A. The power dissipation from the battery for controller and actuators are 7.2V and 14.4V respectively. The actuators of the cleaning robot are DC servo motors for driving the wheels; and DC motor for robot turn mechanism [9]. Figure 2.6 is shown the block diagram of the window cleaning robot control system.

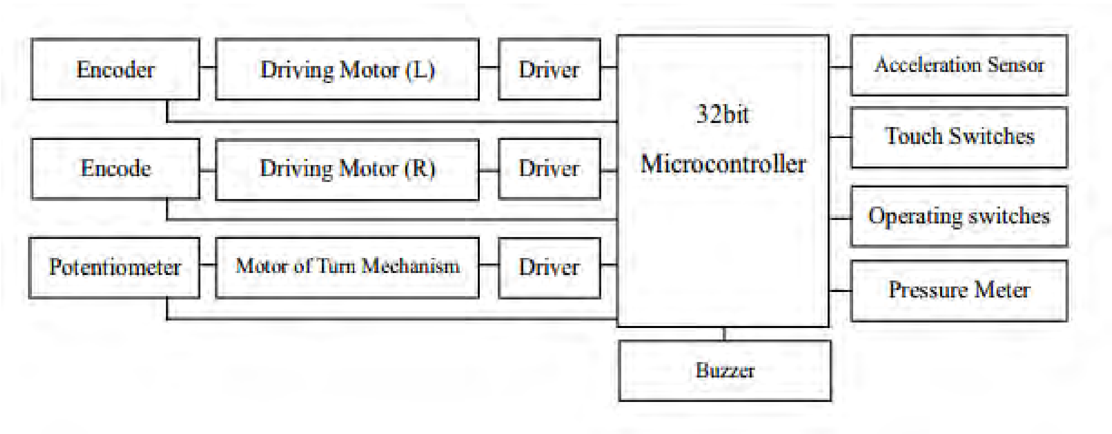

Figure 2.6: Block diagram of the control system [9].

Meanwhile, another type of window cleaning robot had been constructed for domestic used. This cleaning robot is developed using four suction cups as moving mechanism to perform the cleaning task on window glass, drove by radio control (RC) servo motor and driving motor [10]. A vacuum sensor is used to measure the gauge pressure of the suction cups when holding the robot on the window glass. A rotational cylindrical sponge is used as a cleaning device to wipe the dust on the window [10]. Figure 2.7 is shown the diagram of the window cleaning robot.

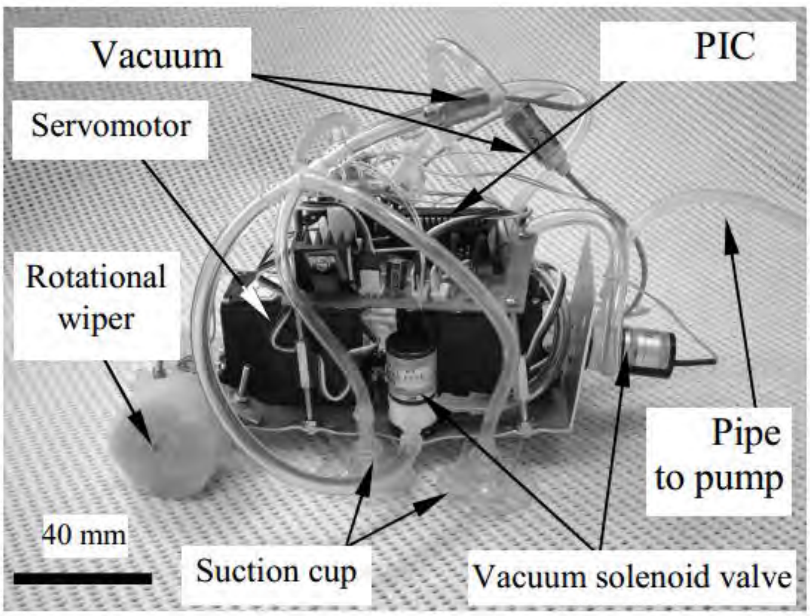

Figure 2.7: View of window cleaning robot [10].

A PIC16F873A microcontroller is implemented in the robot to control the robot system. And also, a 25.9V lithium-polymer battery is used as power supply for the robot [10]. And also, the block diagram of the control system for window cleaning robot control is shown in Figure 2.8.

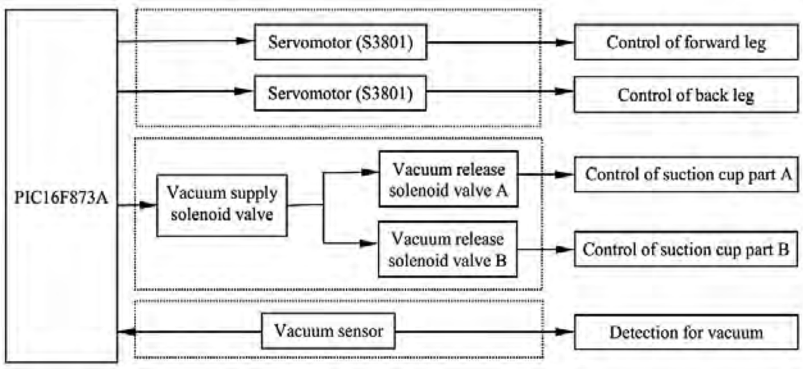

Figure 2.8: Block diagram of window cleaning robot control system [10].

Apart from that, a prototype of the glass cleaning robot is developed by a group of researchers from Nanyang Technological University. This autonomous robot is capable to climb and clean the glasses on a high-rise commercial building. A micro-fiber sponge has been used to clean the glass efficiently. This is because the micro-fiber has electrostatic properties in which it can attach the dust from the glass. This cleaning robot has used HITEC HS-562MC Digital servo motor for the moving motion and D312-7006-5000 vacuum pump is used for holding the robot on the glass. The robot is controlled by BASIC Stamp microcontroller BS-2PE which has 16 inputs and outputs pins. And a nickel metal hydride battery is used as a power source for the robot. A regulator circuit is built to dissipate the power from battery to electronic components accordingly [11]. Figure 2.9 is shown the prototype of the glass cleaning robot.

Figure 2.9: Prototype of glass cleaning robot [11].

Table 2.1: Summary of design components for cleaning robot.

	Journal 1	Journal 2	Journal 3	Journal 4	Journal 5
Title	Autonomous Cleaning Robot: Roboking System Integration and Overview [6]	Building a Mobile Robot for a Floor-Cleaning Operation in Domestic Environments [8]	Development of Small-Size Window Cleaning Robot [9]	A Small Window-Cleaning Robot for Domestic Use [10]	Design and Development of a Glass Cleaning Robot [11]
Cleaning Equipment	Rotating brushes , vacuum	Karcher electric broom	Vacuum	Rotational wiper (cylindrical sponge)	Sponge and micro-fiber components
Power Supply	Nickel Metal Hydride battery - 12 V / 3 Ah	Lead battery - 6 V, 1200 mA	Lithium-polymer battery - 30A max current	Lithium-polymer battery - 25.9V - 11 Ah	Nickel Metal Hydride battery

Controller	Texas Instruments 320LF2406A digital signal processor - 40 MHz - 40 MIPS	Micro-controller - 256 Kb memory - I2C EEPROM	PC 104 (CPU Pentium 166 MHz)	PIC16F873	BASIC Stamp micro-controller BS-2PE
Actuators	5 x DC Motors - 12 V, 70W Servomotor 2 x Encoder (Propelling motor)	Maxon DC geared motors - 12 V - 73 : 1	Wheel driving: 2 x DC servo motors Turn mechanism: DC motor - 1000 L/h flow rate - 800 mbar pressure - 500 g weight	Radio control servomotors (Futaba Co. : Model S3801) - stall torque: 11.2 kg.cm	HITEC HS-562MC Digital Servos

Sensors	14 x Ultrasonic sensors - ultrasonic frequency: 40 kHz 4 x Infrared distance sensor 4 x Infrared seeking 2 x Tactile sensor	Floor sensors: Infrared sensors Collision sensors: Mechanical contact sensors Distance sensors: Ultrasonic sensors (Polaroid 6500 Series electrostatic transducers) - ± 15° beam - range 25 to 1300 cm	Touch switch Acceleration sensor: - Input range : ± 2g ± 5% - Zero g drift : ± 30 mV - Sensitivity : 1 V/g ± 5% - Non-linearity : ± 2% FS - Noise densiy : 140 µg/Hz1/2 - Noise : 1.0 mg rms - Bandwidth : DC -50 Hz ± 5%	Vacuum sensors / Pressure sensor (SMC CO.: Model PSE533) - output signal: 1 V to 5 V - gauge pressure range: -101 to 101 kPa	N/A

		People sensor : Passive infrared sensors with the adequate Fresnel lens	- Dimensions : 19.8 X 44.5 X 27.2 mm (W x D x H) - Weight : 46 gm		
Advantages	The cleaning robot can navigate automatically by using several ultrasonic sensors. Simple cleaning device to perform the cleaning operation.	Maxon DC geared motor can generate high torque to move the robot	The corner of windowpane can be clean by turn mechanism implemented. Lightweight and portable even installed with battery.	Use basic microcontroller can be programmed using C language. Use simple cleaning equipment for cleaning.	Micro-fiber components can wipe the dust easily. Simple design structure.

Disadvantages	The controller used needed to learn its programming language.	The cleaning device is expensive to be implemented.	The controller is expensive to be implemented. Capable to suck up the dust but cannot perform wiping process.	The robot is not stable if the gauge pressure is not balanced among the suction cups.	The turning mechanism is not stable while climbing on the glass.

2.2 Kinematic Analysis

The kinematic analysis for the window cleaning robot has been analysed according to [9]. An attitude angle is measured in a direction of gravity, and also the robot body when the robot is a trajectory to target position. However, the acceleration of the robot is smaller than the acceleration of gravity when the robot is in static or move with a low velocity. Therefore, the attitude control will not be considered the effect of acceleration of the robot in order to measure the acceleration of gravity [9]. A kinematic model for differential-drive robot expressed the relationship between robot angular velocity of attitude and angular velocity of left and right of driving wheels, as shown in Figure 2.10.

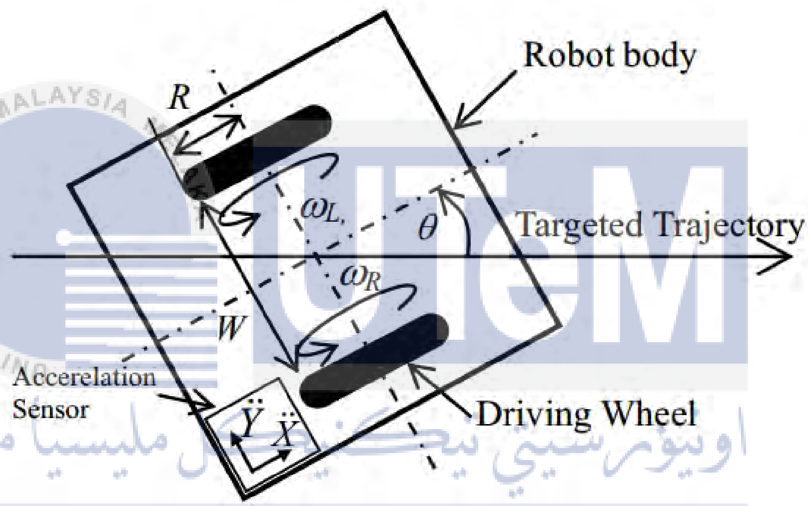

Figure 2.10: Attitude control model with two-wheel locomotion [9].

$$\begin{pmatrix} V \\ \dot{\theta} \end{pmatrix} = \begin{pmatrix} R/2 & R/2 \\ R/W & -R/W \end{pmatrix} \begin{pmatrix} \omega_L \\ \omega_R \end{pmatrix} \tag{2.1}$$

where V is the travelling velocity,

$\dot{\theta}$ is angular velocity of robot attitude,

ω_L and ω_R are the rotational velocity of left and right wheels,

W is the tread,

R is the radius of wheel.

In addition, Equation 2.1 can be applied in controller to control the attitude angle of the robot. Figure 2.11 is shown the block diagram of attitude control for the robot during moving motion.

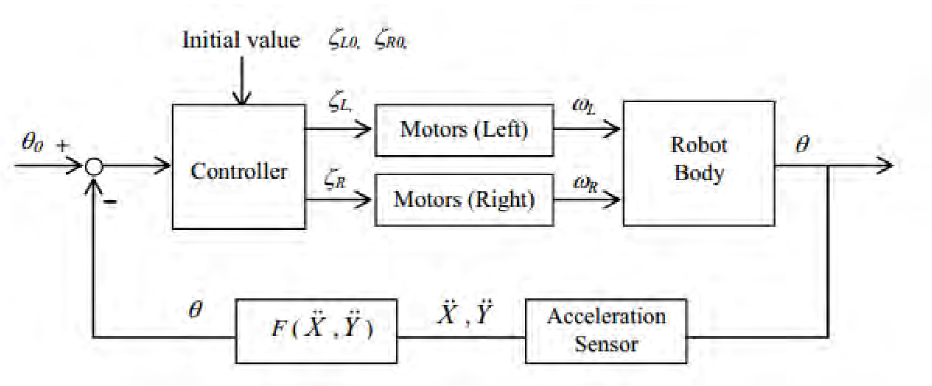

Figure 2.11: Block diagram of attitude control [9].

$$\begin{pmatrix}\zeta_L\\ \zeta_R\end{pmatrix} = \begin{pmatrix}K_P(\theta-\theta_0) & 1\\ 1 & K_P(\theta-\theta_0)\end{pmatrix}\begin{pmatrix}\zeta_{L0}\\ \zeta_{R0}\end{pmatrix} \tag{2.2}$$

where ζ_L and ζ_R are the output duty rate of PWM motor control,

ζ_{L0} and ζ_{R0} are the initial velocity of robot travelling expressed as duty rate,

K_P is the feedback gain.

2.3 Literature Review Conclusion

Based on Table 2.1, the component selection for fan cleaning robot can be reviewed from the summary of the cleaning robot construction from previous researchers. Most of the cleaning robots developed using the rechargeable battery as their power source. Once the battery is low, users need to recharge the robot"s battery at the recharge station. Besides that, DC servo motor and DC motor are mainly used as an actuator to actuate the robot to move and perform the cleaning task. DC motor with higher torque is preferable so that it can drive the robot move around for cleaning operation. However, the ceiling fan cleaning robot proposed will be used 5V DC power supply from the power adapter and DC motor with gear train as the main actuator. And also, Arduino microcontroller will be used to implement in the fan cleaning robot, which is different from the microcontroller used by the previous researchers.

On the other hand, suitable analysis method can be done for this project. Kinematic analysis in term of locomotion can be done on the robot to analyse the moving motion on fan blade. Next, the design and mechanism of the development of robot are discussed in the next chapter.

CHAPTER 3

METHODOLOGY

The ceiling fan cleaning robot is integrated with infrared sensor and limit switch to detect the edge of the fan blade. These electronic components are used to prevent the robot fall down from fan blade. In addition, DC motor with gears is used as an actuator for the robot to move on fan blade, and rotate the roller brushes for cleaning purpose. All the operations are controlled by an Arduino Leonardo microcontroller, including robot moving motion and cleaning operation.

The structure of the robot is designed using SolidWorks computer software before the robot is constructed and assembly. And also, Proteus ISIS software is used for circuitry simulation to test the electronic circuits designed after loaded with programs onto the Arduino microcontroller board. This step is important to ensure the functioning of the circuit and program developed, and can prevent the damage on hardware from being implemented directly.

On the other hand, the project flowchart in Appendix B indicates the process included to accomplish this project. Final Year Project (FYP) 1 is focused on the software simulation and selection of hardware components, such as actuators and sensors, while FYP 2 is started by design and construction of the ceiling fan cleaning robot. Then, a series of experiments are carried out after the prototype is completely constructed and analyse the results obtained to examine the robot performance in term of locomotion. The conclusion summarizes the overall process and decides whether it meet the objective of this project.

3.1 Phases of Project

Based on the objective developed, this project can be conducted into three phases, which are:

1. To derive the mathematical modelling of fan cleaning robot in term of the centre of mass.
2. To design the fan cleaning robot in application of DC motors as actuators, and works with infrared sensor and limit switches for the moving motion.
3. To analyse the robot performance in term of accuracy and reliability for locomotion on ceiling fan blade.

3.1.1 Phase 1: To derive the mathematical modelling of fan cleaning robot in term of centre of mass.

In phase 1, a free body diagram for the ceiling fan cleaning robot is drawn. A mathematical model to find the centre of mass of fan cleaning robot is derived based on the free body diagram. And also, the mechanical design of fan cleaning robot is drawn using SolidWorks software.

3.1.2 Phase 2: To design the moving mechanism for fan cleaning robot.

In phase 2, the type of DC motor as actuator and equipment used to develop the robot are determined. The sensors chosen are infrared sensor and limit switch to detect the edge of the fan blades; and trigger the program created in the microcontroller. Arduino Leonardo as the main microcontroller to control the system based on the algorithms designed. Proteus ISIS software is used to design the electrical and electronic circuit, and simulation of the circuit is done to determine the function of the circuit.

Figure 3.1 is shown the block diagram of fan cleaning robot to move on the fan blade. Infrared sensor as the input to the system, and the output is the rotation of DC motors. The limit switch is used to send a feedback signal to the microcontroller so that the DC motors can rotate in the reverse direction.

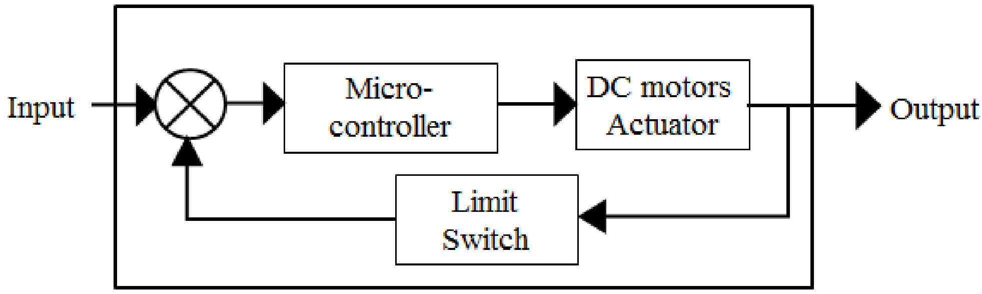

Figure 3.1: Block diagram of fan cleaning robot.

3.1.3 Phase 3: To analyse the robot performance in term of accuracy and reliability for locomotion on fan blade.

In phase 3, a series of experiment are developed to analyse the performance of fan cleaning robot to meet with the expected condition. Analysis is done by comparing the power supply of 6V rechargeable battery and 5V DC power adapter. Experiment on weight of the robot to angle declined of the fan blade, the velocity of the robot and ability of robot move in a straight line by examined the swing angle of locomotion. Data obtained from the experiment are recorded and analysed the performance of fan cleaning robot.

3.1.4 Experimental Design

The focus of the experiment is to achieve the objective of this project:

1. Design and develop a fan cleaning robot,
2. Analysis the performance of fan cleaning robot.

Hence, the criteria for the experiment are determined and a few sets of experiments are being setup. Table 3.1 shown the experiments designed to map with the objective.

Table 3.1: Map of experiments with objective.

Experiment	Objective	
	1	2
1	✖	
2	✖	
3	✖	
4	✖	✖
5		✖
6		✖

Based on Table 3.1, Experiment 1 is about the selection of DC motor, Experiment 2 and Experiment 3 is to examine the sensitivity and accuracy of infrared sensor and digital compass respectively. Next, Experiment 4 is about the angle decline of fan blade from the plane of rotation after the fan cleaning robot is placed on the fan blade; Experiment 5 and Experiment 6 is the determination of velocity and swinging angle of locomotion respectively when the fan cleaning robot is moving in a straight line.

In summary, Experiment 1, Experiment 2 and Experiment 3 are mainly corresponding to the Objective 1, while Experiment 5 and Experiment 6 are corresponding to Objective 2. Meanwhile, Experiment 4 is corresponding to both Objective 1 and Objective 2 at the same time.

3.2 Free body diagram of ceiling fan cleaning robot for derivation of mathematical modelling and mechanical structure design

The system modelling technique is used to find the centre of mass of fan cleaning robot. Derivation of mathematical modelling to find the centre of mass is done so that the robot locomotion performance can be analysed, such as the linear motion and velocity on fan blade [12]. The values of parameters in the derived equation are inserted once the measurement readings are taken from the experiments. And also, SolidWorks software is used to design the mechanical structure of fan cleaning robot.

3.2.1 Equation of the centre of mass for a robot

Figure 3.2 and Figure 3.3 is shown the free body diagram of a four wheels robot moving on a level surface and on an incline plane respectively.

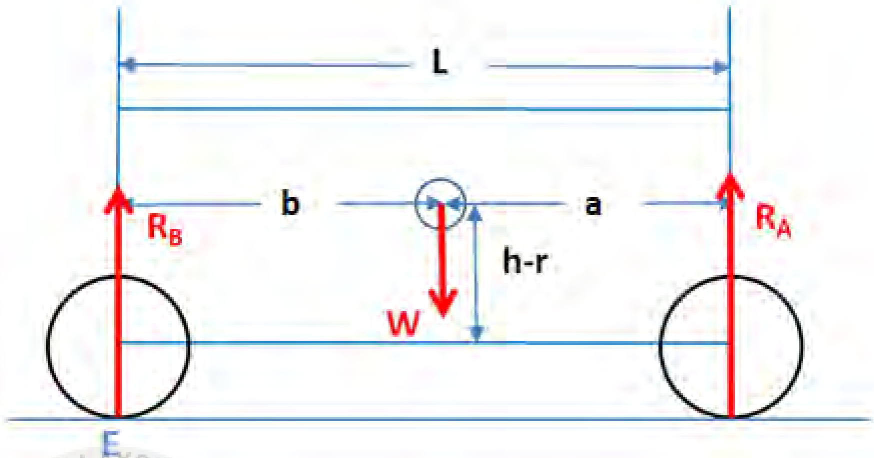

Figure 3.2: Free body diagram of robot on a level surface [13].

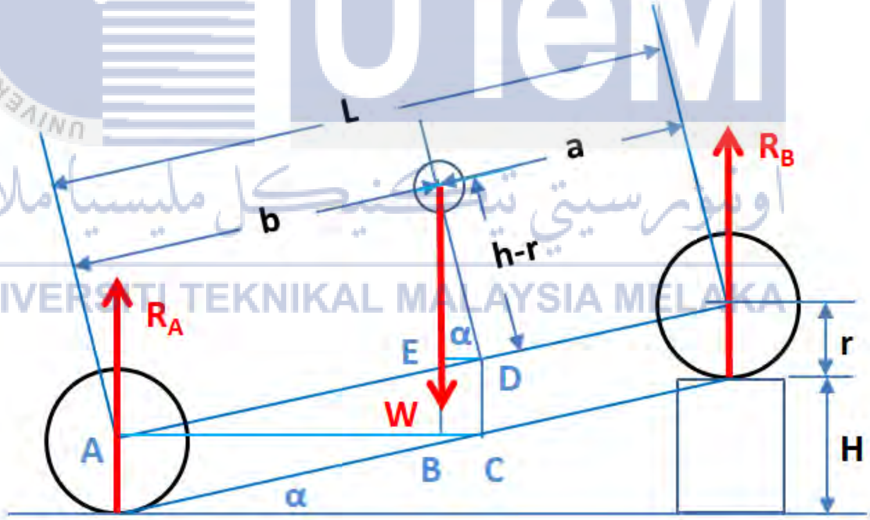

Figure 3.3: Free body diagram of a robot on incline plane [13].

The mass of an object is equally distributed in all directions at the centre of mass. Finding the centre of mass is important where this point can represent the characteristics of an object effectively [12]. The centre of mass is expressed at the x- and y- coordinate respect to the origin. Therefore the centre of mass of the robot as shown in the figure can be determined, by taking the weight and moment about any point on the robot.

Let	α	= Angle of inclination of the plane to the horizontal
	W	= Weight of the robot
	h-r	= Height of the centre of gravity above the axle plane
	H	= Height of incline plane
	r	= Distance between the centres of the wheels to incline plane
	b	= Perpendicular distance of centre of gravity from the rear axle
	a	= Perpendicular distance of centre of gravity from the front axle
	L	= Distance between the centres of the rear and front wheels
	R_A	= Total normal reaction between the ground and the front wheels
	R_B	= Total normal reaction between the ground and the rear wheels

Length of wheel base,

$$L = a + b \tag{3.1}$$

$$a = L - b$$

Summation of vertical forces in the y-direction,

$$\sum F_y = 0$$

$$W - (R_A + R_B) = 0$$

$$W = R_A + R_B \tag{3.2}$$

The robot front axle weight and rear axle weight,

$$W_A = R_A$$

$$W_B = R_B$$

From the Figure 3.2,

Take moments about point E,

$$\sum M_E = 0$$

$$R_A . L + W . b = 0$$

$$R_A . L = W . b$$

$$b = L\left(\frac{R_A}{W}\right) \qquad (3.3)\ [13]$$

From the Figure 3.3,

Take moments about point A,

$$\sum M_A = 0$$

$$R_A . (L\cos\alpha) + W . (A . B) = 0$$

$$R_A . (L\cos\alpha) = W . (A . B) \qquad (3.4)\ [13]$$

$$AB = AC - BC$$

$$AC = b\cos\alpha$$

$$BC = ED = (h - r)\sin\alpha$$

$$\therefore \quad AB = b\cos\alpha - (h - r)\sin\alpha \qquad (3.5)\ [13]$$

Substitute Equation 3.5 to Equation 3.4,

$$R_A . (L\cos\alpha) = W . [b\cos\alpha - (h - r)\sin\alpha]$$

$$W . (h - r)\sin\alpha = W . b\cos\alpha - R_A . (L\cos\alpha)$$

$$h - r = \left[b - L\left(\frac{R_A}{W}\right)\right] cot\,\alpha$$

$$h = \left[b - L\left(\frac{R_A}{W}\right)\right] cot\,\alpha + r \qquad (3.6)\ [13]$$

3.2.2 Mechanical design

The following diagram is the structural design for fan cleaning robot and an extension rod using SolidWorks computer drawing software. The fan cleaning robot has an overall dimension of 38 x 35 x 4.7 (length x width x height) measured in centimetre, and the total weight is about 0.735 kg. Besides, the extension rod is used to place the robot on fan blade. It has dimensions of 11 x 28 x 69 (length x width x height) in centimetre.

The fan cleaning robot is constructed using plywood as its main material. Plywood is lightweight, and can be placed on ceiling fan blade without damage to it. Besides, it is sustainable and easier to be purchased. The benefit of using plywood is because of it is easier to construct the robot by cutting into any suitable design model.

In addition, the extension rod is constructed by using plastic material and has a diameter of 2.2 cm. A base is attached to a long stick for placing the fan cleaning robot on ceiling fan blade. However, this extension rod can be replaced by any long stick with a standard threaded head of diameter.

Figure 3.4 shown the overall of mechanical design for fan cleaning robot, and Figure 3.5 is the top and bottom view for the robot. Figure 3.6 is the diagram of the extension rod designed.

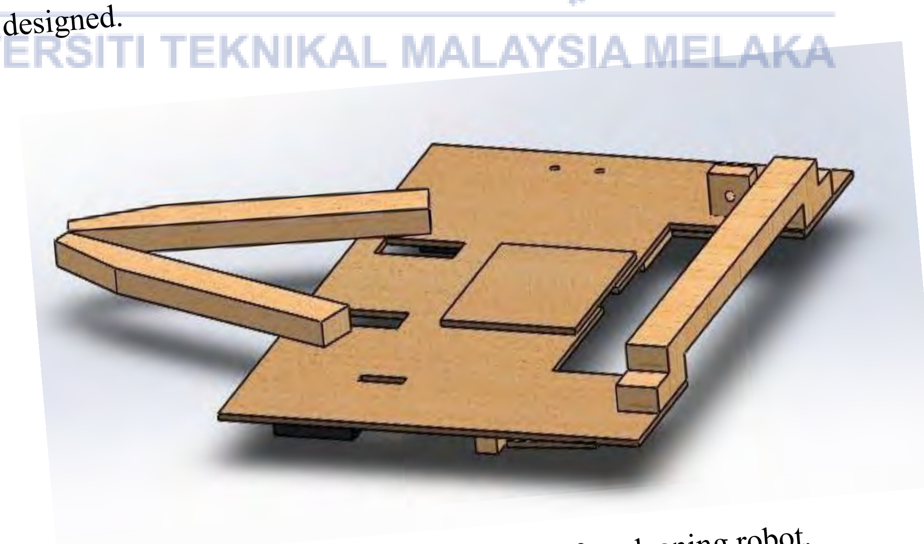

Figure 3.4: Isometric view of fan cleaning robot.

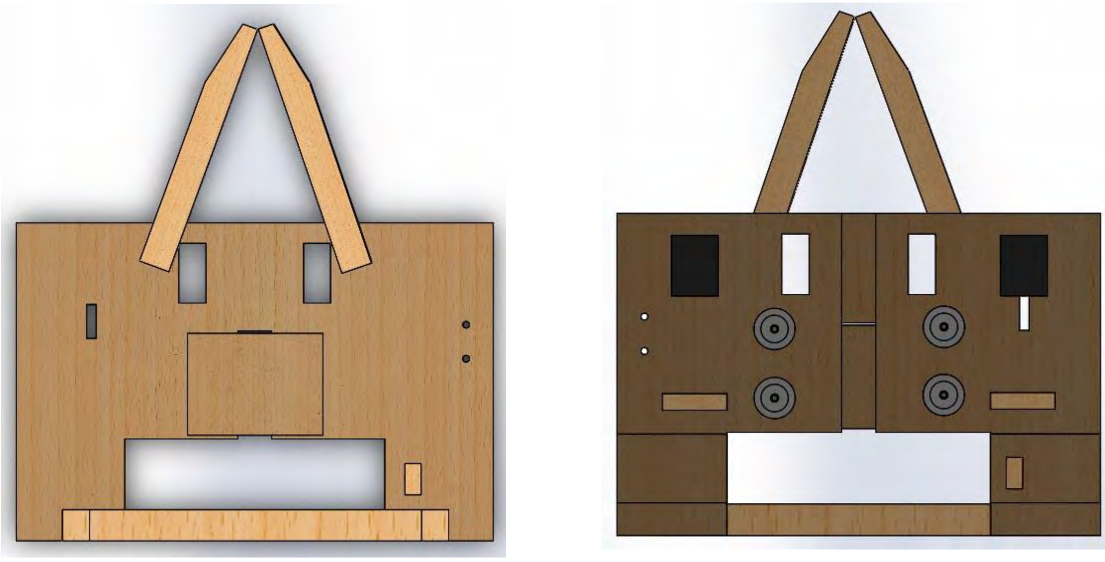

(a) Top view

(b) Bottom view

Figure 3.5: Top view and bottom view of fan cleaning robot.

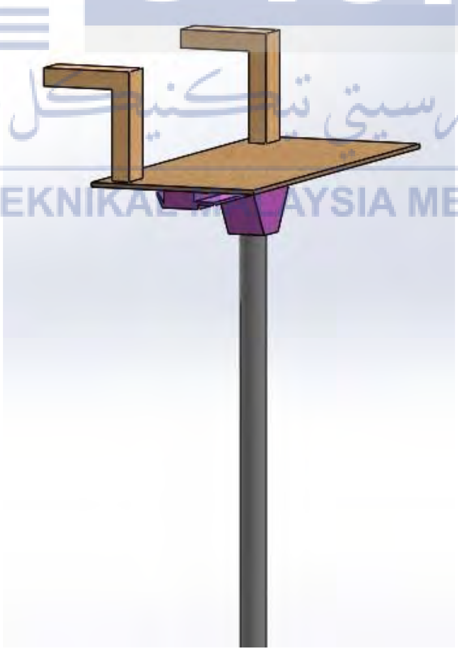

Figure 3.6: Isometric view of extension rod designed.

3.3 Design of moving mechanism for fan cleaning robot in application of DC motors

In this phase, few considerations are taken into account to develop the ceiling fan cleaning robot. This included the selection of actuator and suitable gear train to provide appropriate speed and torque for the robot to move on fan blade, and the equipment needed to assemble the robot. Next, the electrical circuit for the system is designed, and the program designed is loaded onto the Arduino Leonardo microcontroller board integrated with infrared sensor and limit switches to control the operation of the robot. Later, simulation of circuitry designed is carried out to determine the function of the circuit.

In addition, the necessary connection and a program to connect electronic components with Arduino microcontroller are being studied. The Arduino Leonardo microcontroller is chosen in this project due to its characteristics over other Arduino boards. Arduino Leonardo microcontroller implemented ATmega 32u4 as its processor, 16Mhz CPU clock speed, 2.5KB of SRAM, 1KB of the EEPROM and 32KB of flash memory for storing code. It also has 20 digital I/O ports and 12 analog I/O ports respectively, which is enough I/O ports for this project, and it supports native USB transfer [14].

3.3.1 Experiment Test 1: DC motor selection

This experiment is corresponding to Objective 1 of this project, which is to design a fan cleaning robot, by select suitable DC motor as actuators, and design the control algorithms for DC motor.

Objective: 1. To examine the rotational speed of DC motor by adjusting the resistance from the potentiometer.
2. To select a suitable DC motor that able to provide a more reliable speed for moving on the fan blade.

Variables: Independent variable : Resistance applied from potentiometer
Dependent variable : Rotational speed of DC motor

Type of DC motor

Figure 3.7 is shown three models of DC motors. The specification of these DC motors is summarized in Table 3.2 with different operation speed and torque.

Figure 3.7: Mitsumi M31E-1, FC-130SA-2270, Tamiya #70168 double gearbox. [15, 16, 17]

Table 3.2: Specification of three different models of DC motor. [15, 16, 17]

Specifications	**Mitsumi M31E-1**	**FC-130SA-2270**	**Tamiya #70168 double gearbox**
Rated voltage (V)	6	3	3
Torque, mN-m	5.88	1.37	223.19
Operation Speed, rpm	3000	10740	38

Figure of experimental setup

Figure 3.8 is shown the experimental setup for testing the DC motor; and an Arduino Leonardo microcontroller after loaded with the program designed.

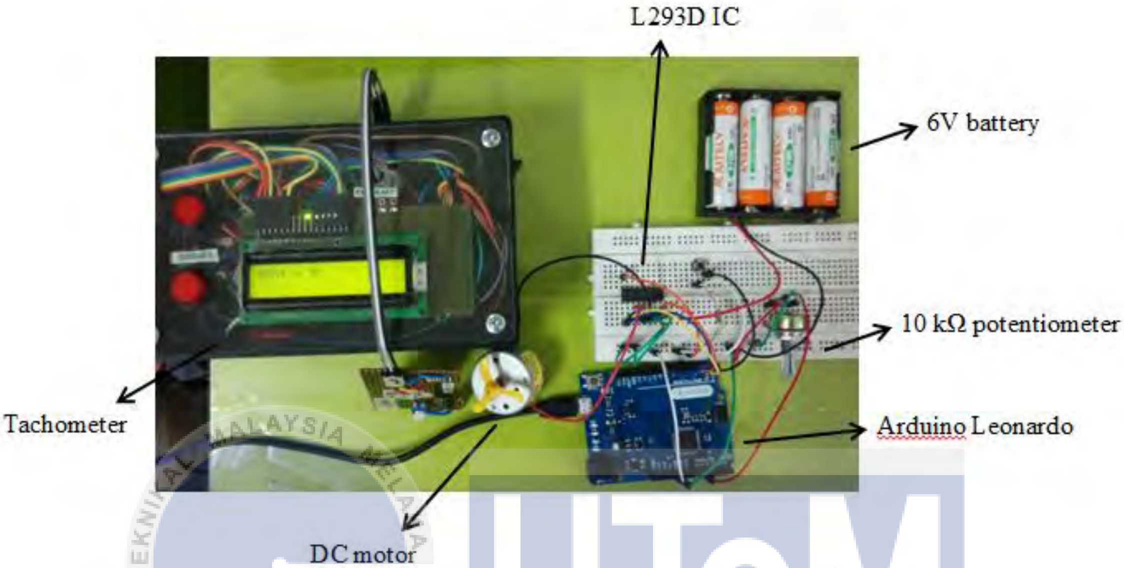

Figure 3.8: DC motor circuit.

Equipment

1. Arduino Leonardo microcontroller
2. Mitsumi M31E-1
3. FC-130SA-2270
4. Tamiya #70168 double gearbox
5. L293D IC
6. 10 kΩ potentiometer
7. 6V battery
8. Tachometer

Procedure

1. The DC motors are supplied with 5V from the Arduino board to determine the spinning direction.
2. A L293D IC is used to control the rotational direction of DC motors. Three pins of L293D: Pin 1 (Enable), Pin 2 (In1) and Pin 7 (In2) are connected to Pin 10, Pin 9 and Pin 8 of the Arduino board; and Pin 3 (Out1) and Pin 6 (Out2) connected to the motor.
3. The program for the motor control is loaded onto the Arduino Leonardo microcontroller board.
4. The DC motor is started to rotate and tachometer is used to measure the rotational speed.
5. Step 1 to step 6 are repeated for the other DC motor. The results are obtained and tabulated in a table.

Formula used in experiment

Mean $= \frac{\sum_{i=1}^{n} x_i}{n}$

Standard deviation $\sigma = \sqrt{\frac{\sum_{i=1}^{n}(x_i - \bar{x})^2}{n}}$

where, n = number of data point

$\bar{x}$ = mean of all values in the data set

x_i = each value in the data set

3.3.2 Experiment Test 2: Distance measurement

This experiment is corresponding to Objective 1, which is to design the fan cleaning robot by designing the control algorithms for infrared sensor to detect the obstacle. The suitable distance that can generate higher voltage signal is determined.

Objective: 1. To examine the sensitivity of infrared sensor in detecting obstacle.
2. To determine the maximum distance can generate higher output voltage

Variables: Independent variable : Distance of the obstacles from infrared sensor

Dependent variable : Output voltage from infrared sensor

Figure of experimental setup

Figure 3.9 is shown the experimental setup for infrared sensor. The infrared sensor is fixed at its position and the obstacle is moved near to it.

Figure 3.9: Infrared sensor circuit.

Equipment

1. Arduino Leonardo microcontroller
2. IR phototransistor
3. IR LED
4. 33 Ω resistor
5. 100 kΩ resistor
6. Multimeter
7. Ruler
8. White paper

Procedure

1. A small piece of electrical tape is cut and wrapped around the IR phototransistor to prevent received light from the sides.
2. The anode pin of the IR LED and IR phototransistor is connected to a 33 Ω resistor and 100 kΩ resistor respectively from 5V power supply, while the cathode pin is connected to ground.
3. A jumper is connected in parallel with IR phototransistor to A0 analog pin on the Arduino board. Then, the program is loaded onto Arduino board.
4. A white paper as obstacle is placed 30 cm away from the infrared sensor, and moved every 2 cm closer to the infrared sensor for 16 times.
5. A multimeter is connected parallel to IR phototransistor to measure the output voltage for every distance, and the result obtained is recorded.
6. Total of 3 sample data are obtained and the average value is calculated.

Formula used in experiment

Mean $= \frac{\sum_{i=1}^{n} x_i}{n}$

Standard deviation $\sigma = \sqrt{\frac{\sum_{i=1}^{n}(x_i - \bar{x})^2}{n}}$

where, n = number of data point

$\bar{x}$ = mean of all values in the data set

x_i = each value in the data set

3.3.3 Experiment Test 3: Accuracy test of digital compass

This experiment is corresponding to Objective 1, which is to design the fan cleaning robot by designing the control algorithms for digital compass. The data obtained is to determine the accuracy of a digital compass.

Objective: To examine the accuracy and precision of digital compass over position.

Variables: Independent variable : Position of the digital compass reference to the angle on a protractor

Dependent variable : Angle measured from the digital compass in term of azimuth bearing

Figure of experimental setup

Figure 3.10 is shown the connection of a digital compass to Arduino board. A protractor is placed on a white paper and the angle is drawn on it accordingly.

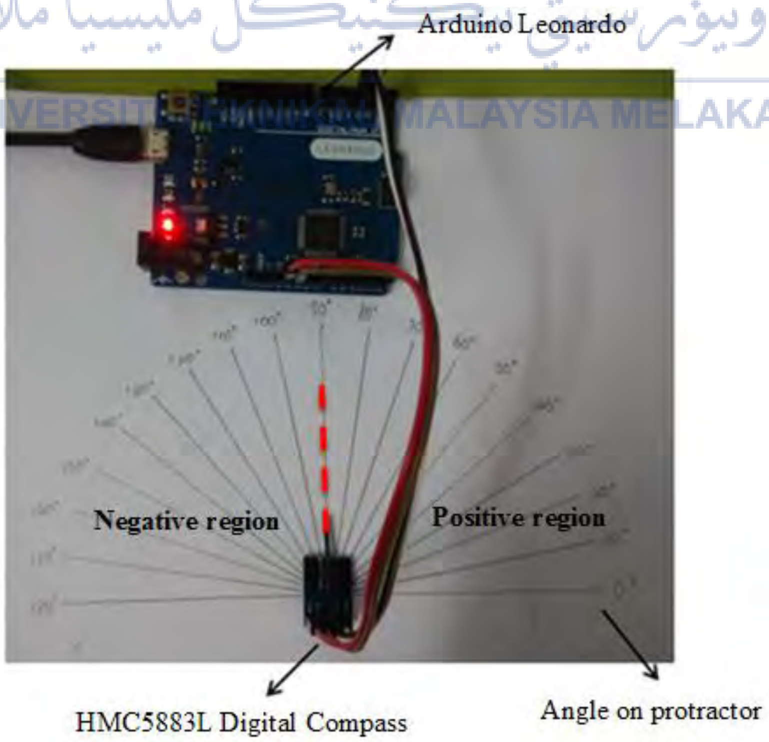

Figure 3.10: Digital compass connection.

Equipment

1. Arduino Leonardo microcontroller
2. HMC5883L Digital Compass
3. Protractor
4. White paper

Procedure

1. A protractor is placed on a white paper and the position angle is drawn accordingly.
2. The HMC5883L digital compass is connected to the Arduino board. Pin from digital compass: VCC, GND, SCL and SDA are connected to pin 5V, GND, SCL and SDA respectively on the Arduino board.
3. The program is loaded onto Arduino board and the initial azimuth bearing measured by digital compass is recorded.
4. The range of digital compass is turned from 0° to -90°, and then from 0° to 90°.
5. The digital compass is turned every 10° for 19 times based on the protractor and the results obtained are recorded.
6. Total of 3 sample data are obtained and analysed.

Formula used in experiment

Mean $= \frac{\sum_{i=1}^{n} x_i}{n}$

Root Mean Square Error $RMSE = \sqrt{\frac{1}{n}\sum_{j=1}^{n}\left(y_j - \hat{y}_j\right)^2}$

where, n = number of data point

$\bar{x}$ = mean of all values in the data set

x_i = each value in the data set

y_j = measured value

$\hat{y}_j$ = expected value

3.3.4 Control system

The operation system for fan cleaning robot is controlled by Arduino Leonardo microcontroller after the program designed is loaded onto the microcontroller board. Basically, there are two inputs for the robot, which is mechanical switches to turn on and off of the robot, and the program created as the database in the microcontroller. Then, the output is the rotation of a DC motor to actuate the robot. Figure 3.11 is shown the block diagram of the control system in fan cleaning robot, which consists of input and output components with the controller.

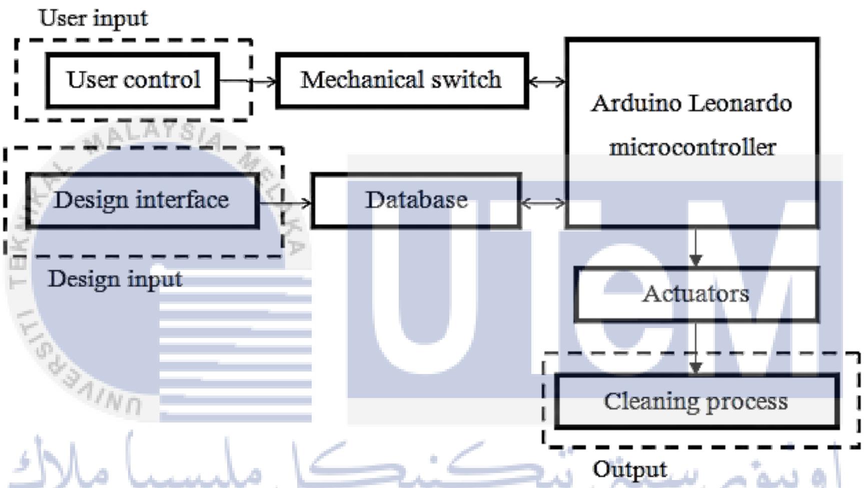

Figure 3.11: Block diagram for the control system in fan cleaning robot.

The electrical circuitry for fan cleaning robot is designed using Proteus ISIS computer software. Figure 3.12 is shown the schematic diagram of electrical circuit for fan cleaning robot developed in Proteus ISIS. This electrical circuit is mainly used for simulation to determine the functional and practical of the circuit designed in accordance with the program developed.

In the electrical circuit designed, there are 2 limit switches used to control the robot movement, which is to turn on and off of the robot, and the other limit switch will work with infrared sensor to detect the end part of fan blade, so that the robot can move in forward and reverse direction for the cleaning process. A L293D H-Bridge drive is used to control the rotation direction of 4 DC motors. All the operation is controlled by Arduino Leonardo microcontroller after the program is loaded.

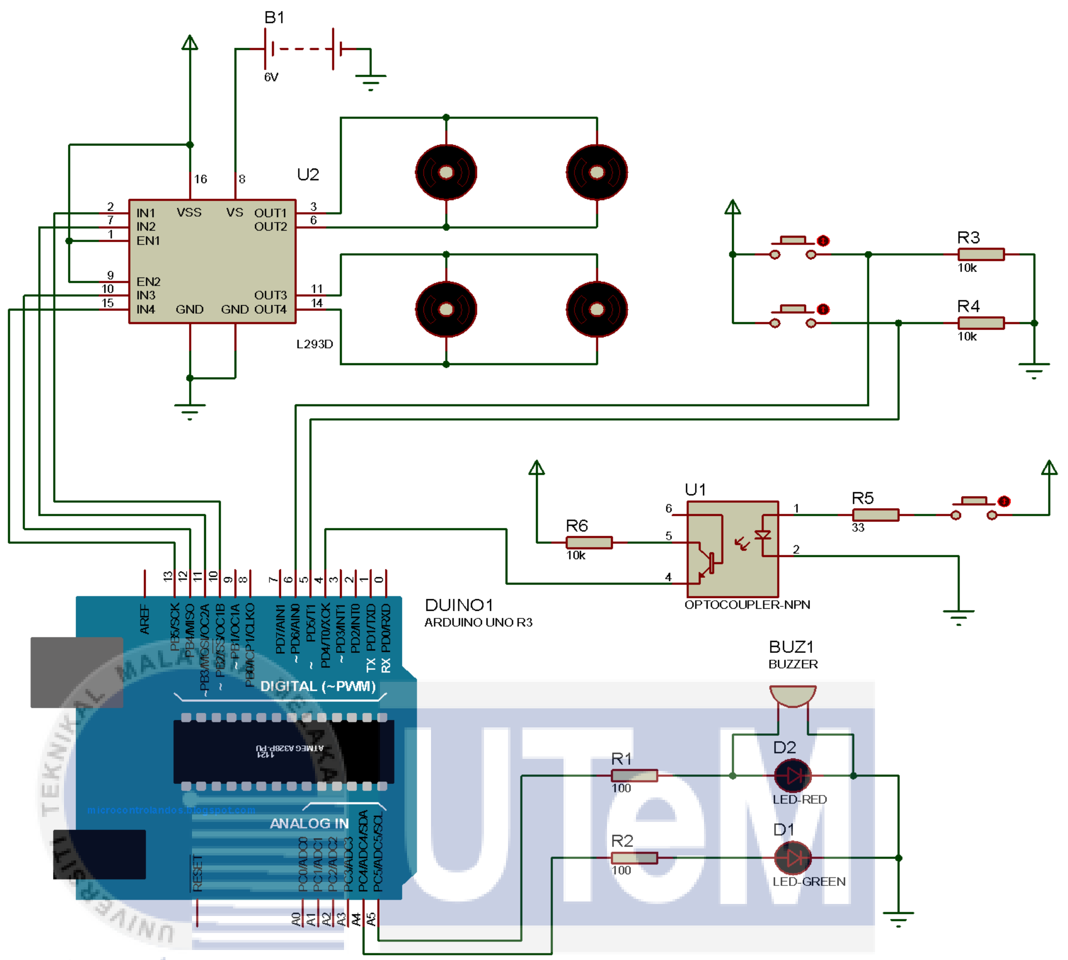

Figure 3.12: Schematic diagram of electrical circuit design.

Figure 3.13 is shown the algorithm flowchart to operate the fan cleaning robot. The fan cleaning robot is activated when the On/Off switch is triggered, and then a Green LED is turned on. Then, a situation is occurred to select which of the input state is true. The robot will be moved in a forward direction if the infrared sensor at the back of the robot is triggered, where it does not detect the fan blade. Next, the robot will be moved in reverse direction after the infrared sensor detected the f an blade and front limit switch is triggered by touching the canopy of the ceiling fan. This process will be looped twice and stop automatically. Red LED and buzzer will be turned on to indicate the robot is stopped.

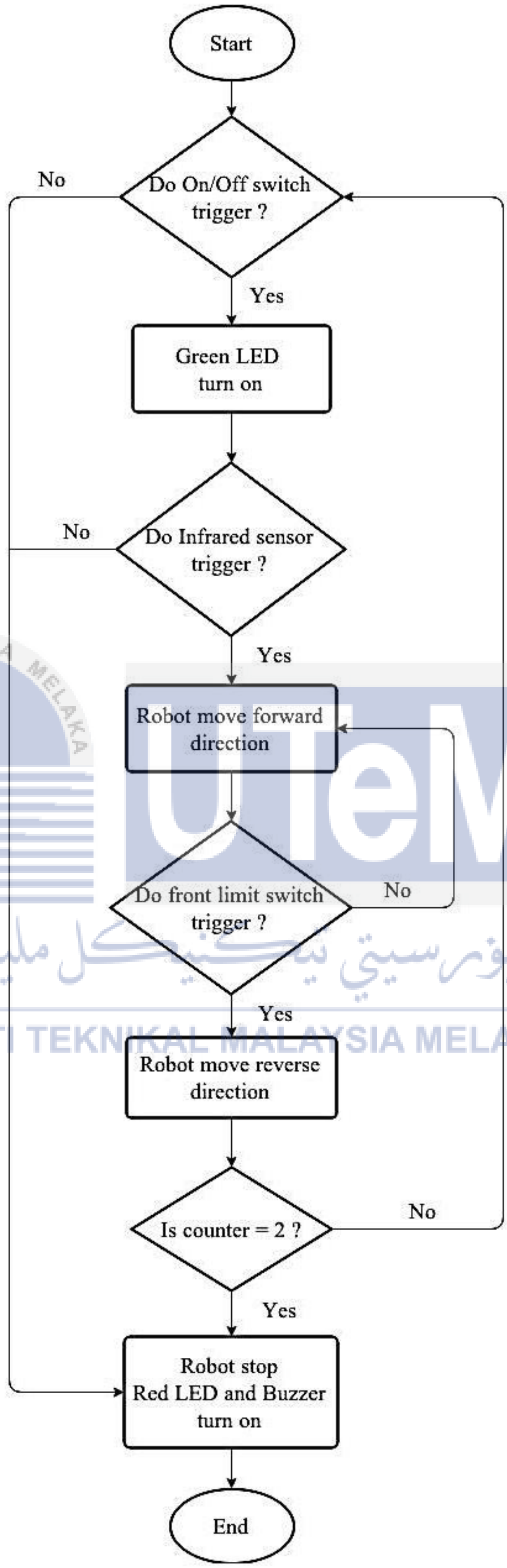

Figure 3.13: Algorithm to actuate the fan cleaning robot.

3.4 Analyse the robot performance in term of accuracy and reliability for locomotion on fan blade.

Three sets of experiments are done to analyse the performance of fan cleaning robot by comparing the power supply to the robot, which is 6V rechargeable battery and 5V DC power adapter. Experiments included are to determine the angle decline from the plane of rotation of the fan blade, velocity of the robot moving on fan blade, and the swinging angle deviated from a straight line while the robot is moving on fan blade.

3.4.1 Experiment Test 4: Angle decline of fan blade

This experiment is corresponding to Objective 1 and Objective 2, which is to design and develop the fan cleaning robot, and analyse the robot locomotion when the robot is moving on fan blade. This experiment is to determine the effect of weight of robot to the ceiling fan blade.

Objective: To determine the declination angle of fan blade being pushed down by fan cleaning robot by comparing the weight of the robot.

Variables: Independent variable : Weight of fan cleaning robot
Dependent variable : Declination angle

Figure of experimental setup

Figure 3.14 and Figure 3.15 is shown the position of the angle taken to determine the declination angle of fan blade after pushed down by fan cleaning robot.

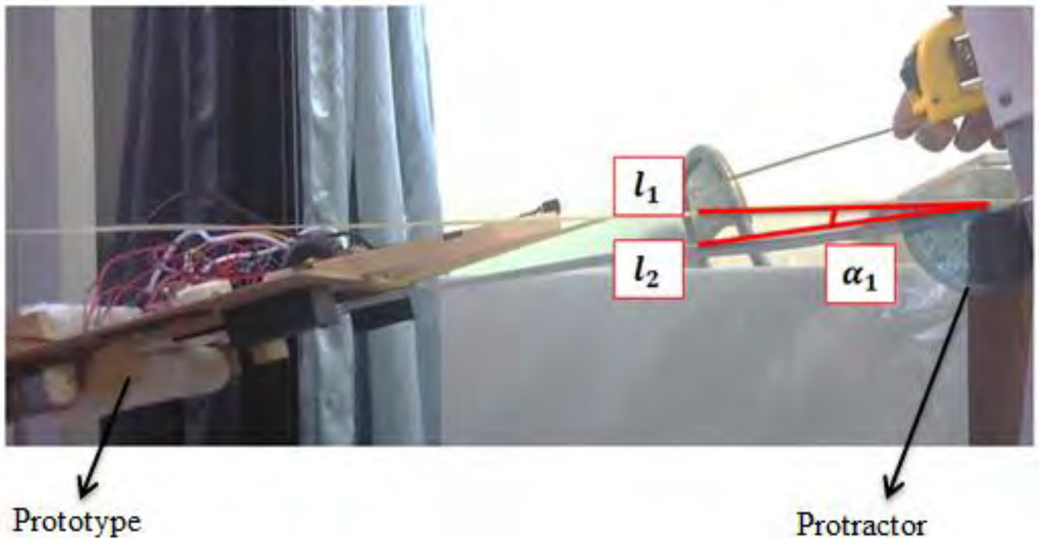

Figure 3.14: Angle declination α_1 at the motor housing of ceiling fan.

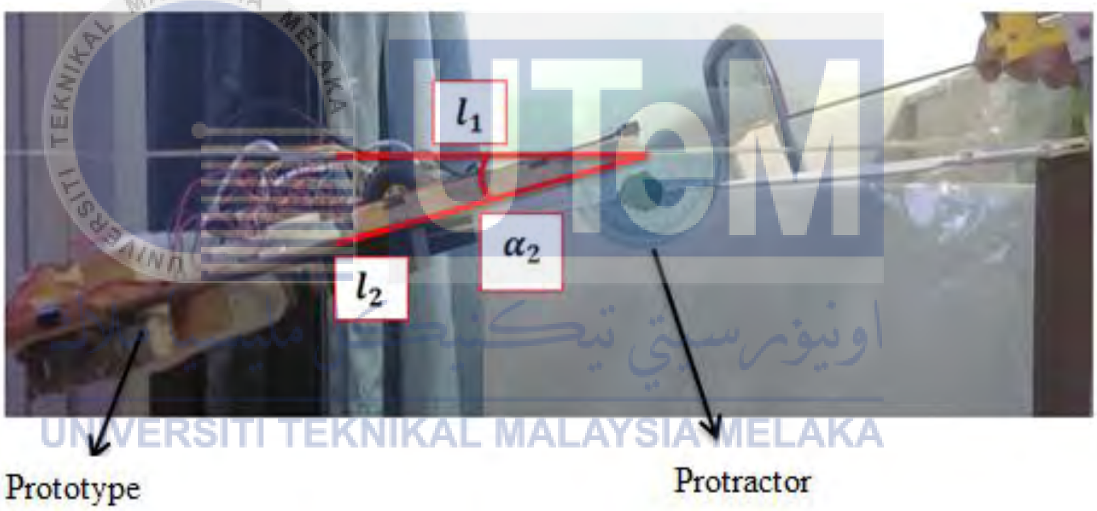

Figure 3.15: Angle declination α_2 at the end of fan blade.

Equipment

1. 6V rechargeable battery
2. Fan cleaning robot prototype
3. Ceiling fan blade
4. Digital weight scale
5. Protractor
6. Measuring tape

Procedure

1. The weight of fan cleaning robot with 6V rechargeable battery is measured using digital weight scale and recorded.
2. Two protractors are placed at different position with the fan blade respect to the plane of rotation.
3. The blade is being pushed downward after the fan cleaning robot is placed at the end of fan blade.
4. The declination angle, α_1 and α_2 are measured by taking the tangent of fan blade in curve shape, l_2 intercept with the plane of rotation, l_1 and the reading is recorded.
5. Step 3 and 4 are repeated for 5 times to obtain the average value of declination angle.
6. Step 1 is repeated to measure the weight of robot without 6V rechargeable battery. Step 5 is repeated and the results obtained are recorded.
7. The data is analysed and a graph is plotted.

Formula used in experiment

Mean $= \frac{\sum_{i=1}^{n} x_i}{n}$

Standard deviation $\sigma = \sqrt{\frac{\sum_{i=1}^{n}(x_i - \bar{x})^2}{n}}$

where, n = number of data point

$\bar{x}$ = mean of all values in the data set

x_i = each value in the data set

3.4.2 Experiment Test 5: Velocity of fan cleaning robot

This experiment is corresponding to Objective 2, which is to analyse the robot locomotion while moving on fan blade. The speed of fan cleaning robot is determined in this experiment.

Objective: To determine the velocity of fan cleaning robot moving on fan blade by comparing two different power supplies.

Variables: Independent variable : Time taken to complete 1 cycle (forward and reverse direction)

Dependent variable : Distance travelled by the robot

Figure of experimental setup

Figure 3.16 is shown the experimental setup to measure the velocity of fan cleaning robot on fan blade.

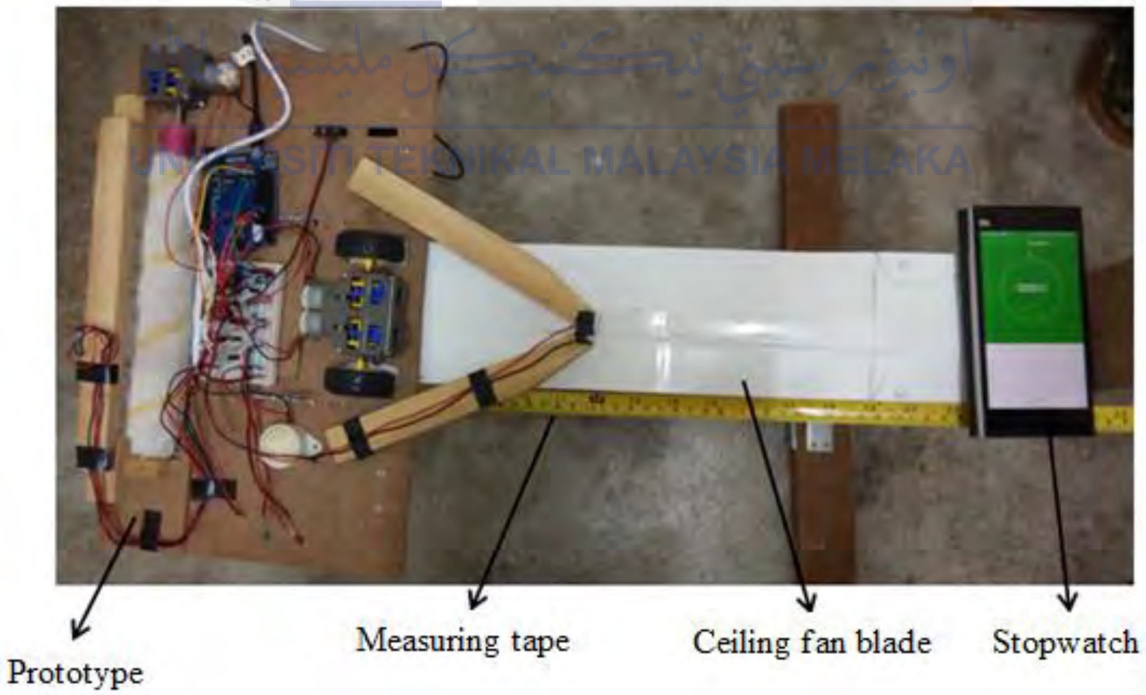

Figure 3.16: Experiment setup to measure velocity.

Equipment

1. Arduino Leonardo microcontroller
2. 6V rechargeable battery
3. 5V DC power adapter
4. Fan cleaning robot prototype
5. Ceiling fan blade
6. Stopwatch
7. Measuring tape

Procedure

1. The length of the ceiling fan blade is measured using measuring tape.
2. A 6V rechargeable battery is used as the power source for fan cleaning robot.
3. The fan blade is sandwiched in the fan cleaning robot and the starting point of the robot is recorded.
4. Stopwatch is used to measure the time taken for the robot to move on fan blade, and the distance travelled by the robot is recorded every second.
5. Step 3 and 4 are repeated for 5 times to obtain the average value of distance travelled.
6. Step 5 is repeated by replacing 6V rechargeable battery to 5V DC power adapter as power supply for the robot.
7. The results of obtained is recorded and tabulated in a table.
8. Data is analysed to examine the velocity of the robot.

Formula used in experiment

Mean $$= \frac{\sum_{i=1}^{n} x_i}{n}$$

Standard deviation $$\sigma = \sqrt{\frac{\sum_{i=1}^{n} (x_i - \bar{x})^2}{n}}$$

where, n = number of data point

$\bar{x}$ = mean of all values in the data set

x_i = each value in the data set

3.4.3 Experiment Test 6: Angle deviated from straight line

This experiment is corresponding to Objective 2, which is to analyse the robot locomotion. When the fan cleaning robot is moving on fan blade, the robot will swing. Hence this experiment can determine the swinging angle from the straight line.

Objective: To examine the ability of fan cleaning robot moving in a straight line on ceiling fan blade

Variables: Independent variable : Time taken to complete 1 cycle of moving on fan blade

Dependent variable : Angle deviated from the straight line

Figure of experimental setup

Figure 3.17 is shown the experimental setup to measure the angle deviated of fan cleaning robot while moving on fan blade. The initial value of azimuth bearing is measured using digital compass and compared with compass.

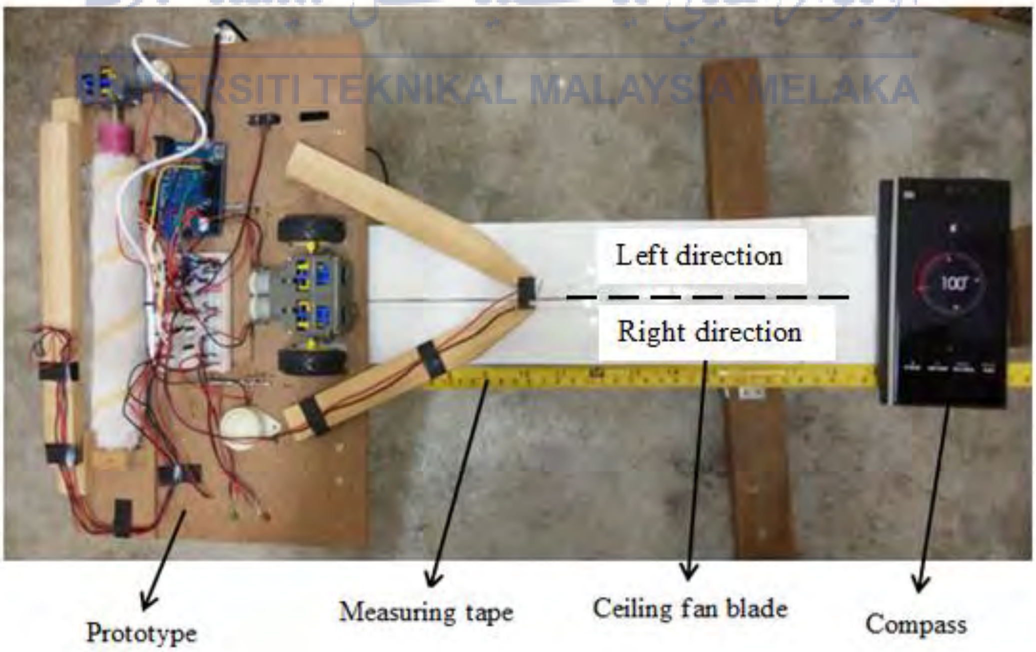

Figure 3.17: Experiment setup for measuring angle from straight line.

Equipment

1. Arduino Leonardo microcontroller
2. 6V rechargeable battery
3. 5V DC power adapter
4. HMC5883L Digital Compass
5. Fan cleaning robot prototype
6. Ceiling fan blade
7. Stopwatch
8. Compass

Procedure

1. The fan cleaning robot is connected with 6V rechargeable battery.
2. The fan blade is sandwiched in the fan cleaning robot and the initial azimuth bearing measured by digital compass is compared with compass.
3. The robot is turned on to move on the fan blade and digital compass is starting to measure the angle deviated from the straight line on fan blade.
4. Step 2 and 3 are repeated for 5 times to take the average angle measured. The data obtained is respect to the time needed for robot to complete 1 cycle of locomotion.
5. Step 4 is repeated by replacing 6V rechargeable battery to 5V DC power adapter.
6. Data is analysed and graphs are plotted.

Formula used in experiment

Mean $= \frac{\sum_{i=1}^{n} x_i}{n}$

Root Mean Square Error $RMSE = \sqrt{\frac{1}{n}\sum_{j=1}^{n}\left(y_j - \hat{y}_j\right)^2}$

where, n = number of data

x_i = each value in the data set

y_j = measured value

$\hat{y}_j$ = expected value

CHAPTER 4

RESULT AND DISCUSSION

This chapter covers the results of experimental tested in the previous chapter. The experiment data are summarized and tabulated in a table. Statistical method is used to analyse and evaluate the data obtained. Then, discussion for each experiment is made according to the results obtained. Next, the derivation of mathematical modelling on a free body diagram of fan cleaning robot is completed with calculation by insert the value of parameters.

4.1 Completed Hardware

Figure 4.1 is shown the complete prototype of the ceiling fan cleaning robot. The fan cleaning robot is integrated with DC motors, limit switches, infrared sensors and Arduino microcontroller. The rubber wheels and rotating brushes are used to enable the robot moving on fan blade and clean the surface of fan blade respectively. The fan blade can be sandwiched between two rotating brushes, so that the brushes can rotate to clean the top and bottom surface of fan blade.

In addition, an extension rod is used to place the fan cleaning robot on the fan blade. It can act as a switch to turn on the robot once it takes down from the robot. Also, LEDs and buzzer are allocated on the robot to indicate the start and stop working on the robot.

Figure 4.2 and Figure 4.3 is shown the top and bottom view of the prototype and Figure 4.4 is the diagram of extension rod prototype.

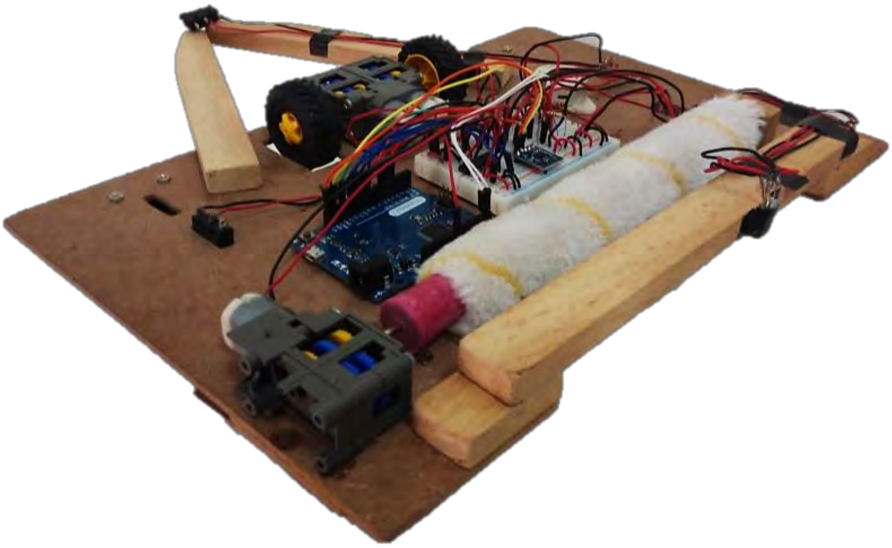

Figure 4.1: Ceiling fan cleaning robot prototype.

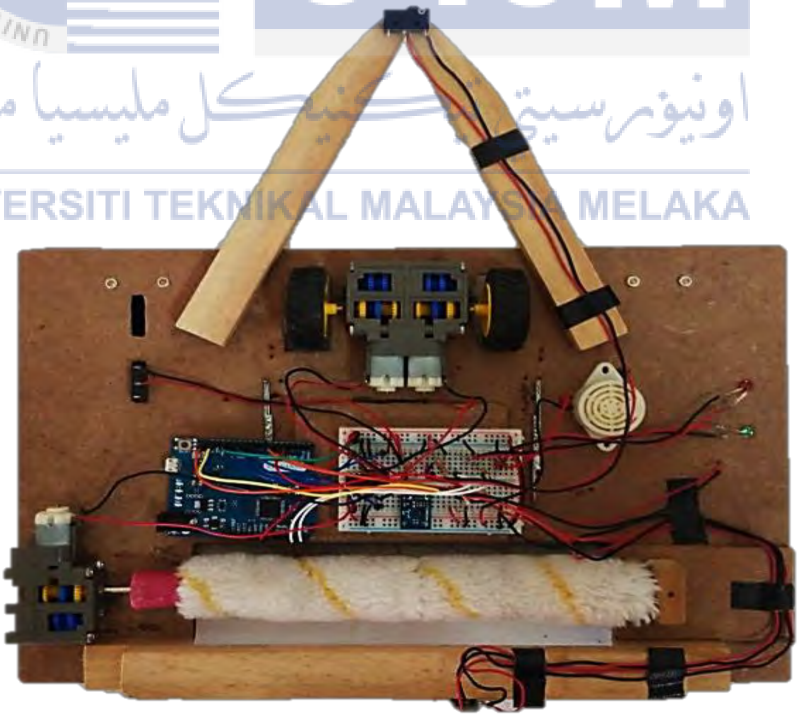

Figure 4.2: Top view of ceiling fan cleaning robot prototype.

Figure 4.3: Bottom view of ceiling fan cleaning robot prototype.

Figure 4.4: Extension rod prototype.

4.2 Experimental Result

4.2.1 Experiment Test 1: DC motor selection

Figure 4.5 is shown the graph of rotational speed on three models of DC motor against the variable resistance. The results and data obtained are tabulated in Appendix C. The DC motor used in this experiment is Mitsumi M31E-1, FC-130SA-2270 and Tamiya #70168 double gearbox.

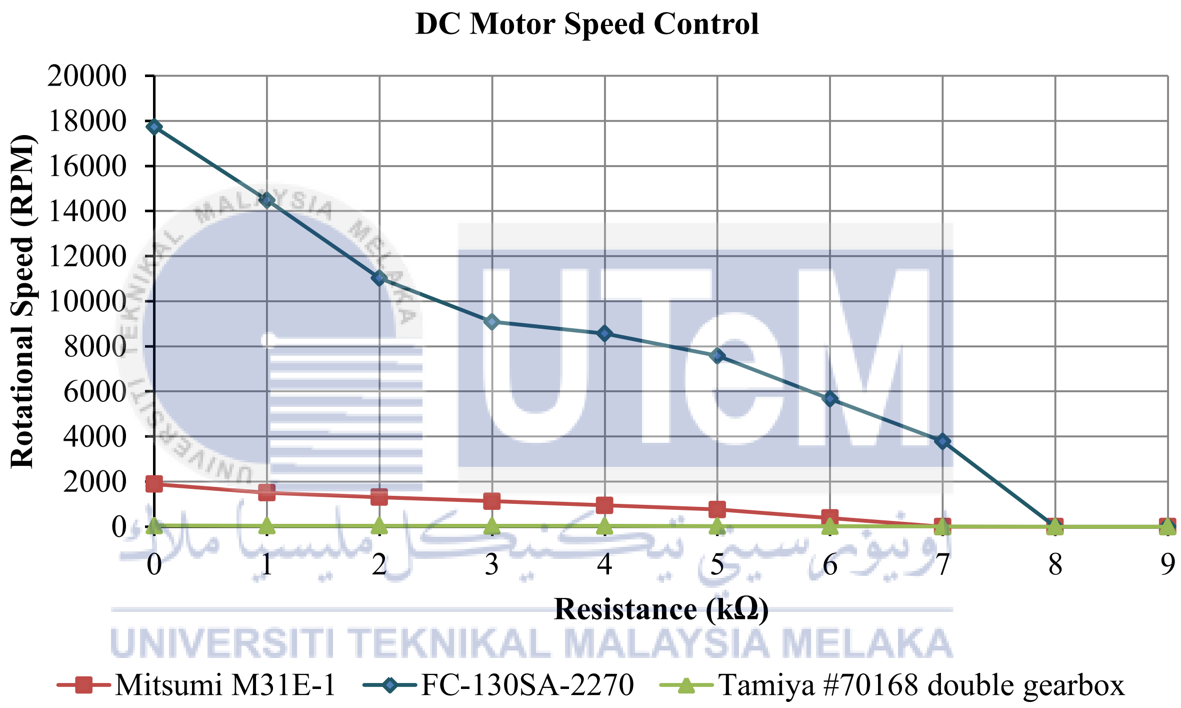

Figure 4.5: Variation of speed against resistance.

Based on the results obtained in Figure 4.5, the rotational speed of three model DC motor is decreased as the increase of resistance in potentiometer. Tamiya #70168 double gearbox is decreased constantly over the resistance applied to it. However, the initial rotational speed for this motor is only 53 RPM, which is lower than the other two models of DC motor. At 7 kΩ before the Tamiya #70168 is stopped, it has a rotational speed of 7 RPM only, which is very low and hard to actuate.

Besides that, the rotational speed of Mitsumi M31E-1 DC motor is shown a gradually decreased as the resistance increased. The initial rotational speed for Mitsumi M31E-1 at 0 Ω is 1887 RPM. At 6 kΩ, its speed is decreased until 384 RPM and stopped at 7 kΩ. For FC-130SA-2270, this motor has a significantly higher rotational speed compared to other DC motor. The initial value of rotational speed for this motor is 17737 RPM and decreased linearly until 11027 RPM at 2 kΩ. However, a non-linear decreasing of rotational speed after 2 kΩ as the resistance applied increased. It has decreased until 3787 RPM at 7 kΩ, and turned down sharply to 0 RPM at 8 kΩ. Meanwhile, all the three models of DC motor are stopped to rotate when the resistance is 8 kΩ. This is because the overall resistance in the armature circuit is increased by increasing the resistance in potentiometer, since the potentiometer is connected in series with the armature circuit and the actual resistance of the armature winding is fixed for the selected motor.

Refer to Appendix C, the standard deviation is calculated from the data obtained. By taking the measured rotational speed for FC-130SA-2270 DC motor at resistance equal to 5 kΩ, the standard deviation can be calculated as below:

$$\sigma = \sqrt{\frac{\sum_{i=1}^{n}(x_i - \bar{x})^2}{n}}$$

$$\sigma = \sqrt{\frac{(7708 - 7583)^2 + (7520 - 7583)^2 + (7520 - 7583)^2}{3}}$$

$$\sigma = 88.6240\, rpm$$

The average speed for this motor at 5 kΩ is 7583 RPM, however, the standard deviation calculated is relatively small. Therefore, the value of standard deviation calculated is closed to the average speed over the resistance applied.

Among three models of DC motor, Tamiya #70168 provide a lower rotational speed, while Mitsumi M31E-1 and FC-130SA-2270 can provide higher speed. Due to the speed is inversely proportional to the torque; a higher torque is obtained at low speed and vice versa. Hence, Tamiya #70168 is suitable to implement in fan cleaning robot due to the robot developed does not require higher speed. But, higher torque is required to enable the robot move on fan blade after the fan blade is pushed down, and the appropriate speed to move on fan blade.

4.2.2 Experiment Test 2: Distance measurement

Figure 4.6 is shown the graph of sensitivity test on infrared sensor based on results tabulated in Appendix D. This experiment is important to determine the suitable distance to locate the infrared sensor on the robot, so that the program can be triggered in the microcontroller and then the robot can be actuated.

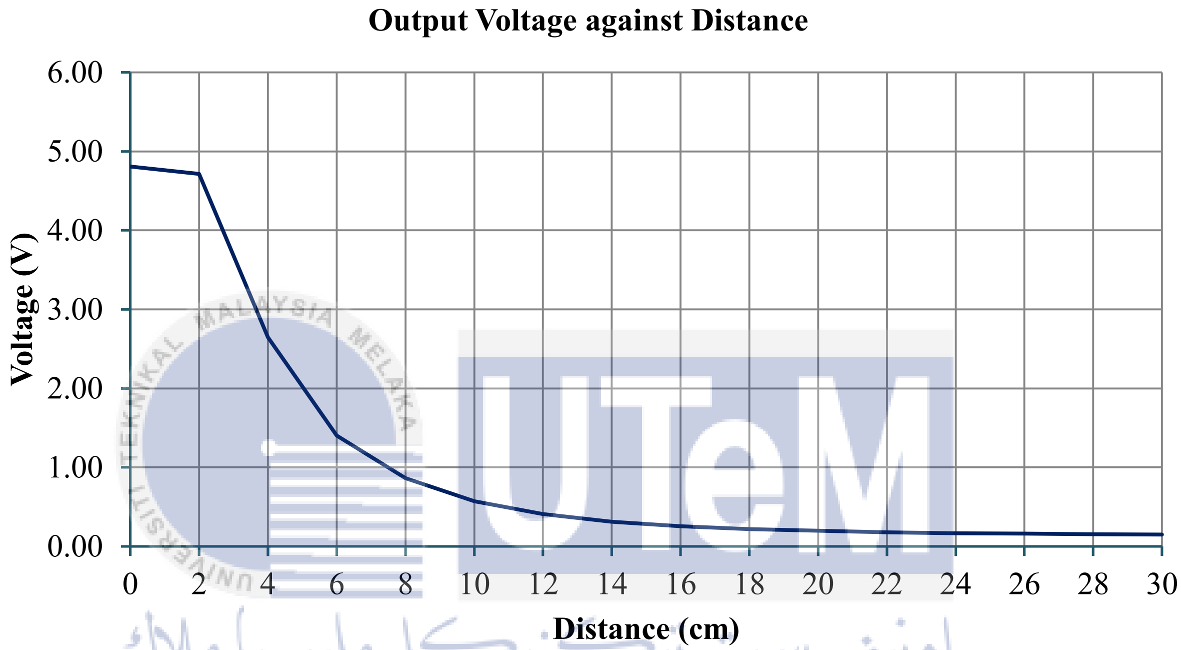

Figure 4.6: Graph of sensitivity test for infrared sensor.

Based on Figure 4.6, the output voltage generated by infrared sensor against the position of the obstacle is plotted. The result obtained for 30 cm length indicated the infrared sensor is responded to only short range distance. Initially the obstacle is located at position 30 cm away from infrared sensor; and the output voltage generated is 0.15 V. However, as the obstacle is approaching and closer to the infrared sensor, the output voltage generated is increasing exponentially, from 0.15 V to 4.72 V at 2 cm. When the obstacle is at position less than 2 cm, the voltage generated is increased slightly from 4.72 V to 4.81 V.

Refer to Appendix D, the standard deviation is calculated from the data obtained. Taking the distance of 10 cm, the standard deviation is calculated as below:

$$\sigma = \sqrt{\frac{\sum_{i=1}^{n}(x_i - \bar{x})^2}{n}}$$

$$\sigma = \sqrt{\frac{(0.59 - 0.57)^2 + (0.56 - 0.57)^2 + (0.57 - 0.57)^2}{3}}$$

$$\sigma = 0.0125\ V$$

As the obstacle reach at 10 cm to infrared sensor, the average output voltage generated is 0.57 V. The value of standard deviation calculated is 0.0125 V, which is tend to be closed to 0.57 V. Hence, the result obtained from the infrared sensor is considered accurate.

In summary, the circuit designed for infrared sensor can be modified to detect the edge of the fan blade as an obstacle. If the IR phototransistor did not receive the signal from IR LED, the generated voltage is low; therefore the robot will be moved in a forward direction. However, the robot will be moved in reverse direction if the condition is met, where the output voltage from infrared sensor is high and front limit switch is triggered.

4.2.3 Experiment Test 3: Accuracy test of digital compass

Figure 4.7 is shown the graph of accuracy test for HMC5883L digital compass. The result for this experiment is shown in Appendix E.

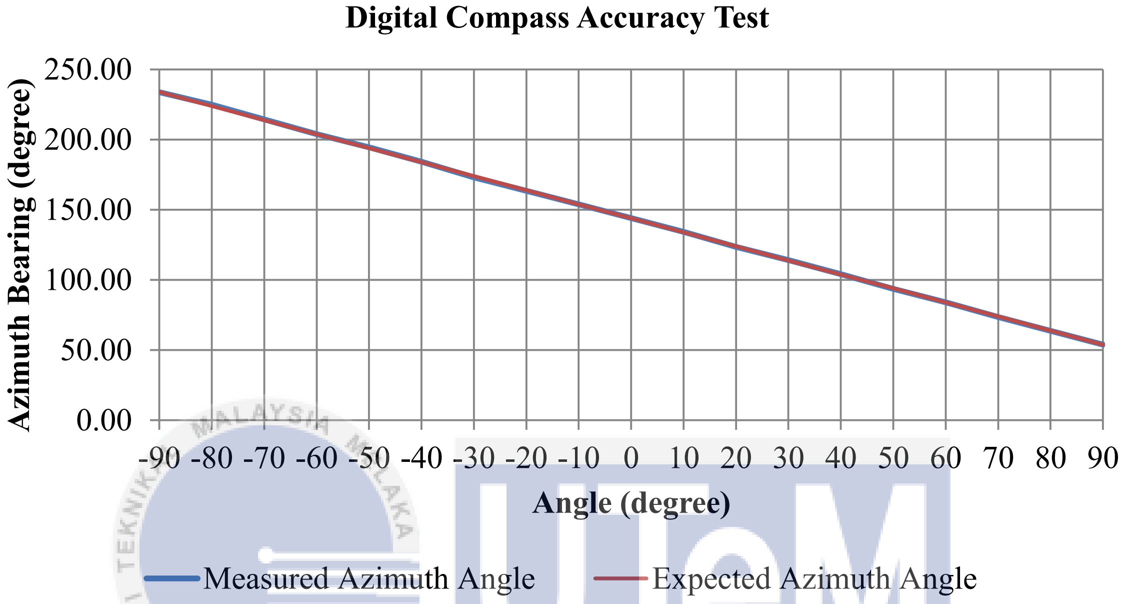

Figure 4.7: Graph of accuracy test on digital compass.

Based on Figure 4.7, the graph is shown the accuracy test on digital compass. From the figure above, the graph is shown a linear relationship of azimuth bearing measured by digital compass and angle of the protractor. The azimuth bearing measured by a compass is heading to the North direction; and is the result of turning for every 10° respect to the angle on the protractor between the ranges of -90° to 90°.

Besides that, this graph is shown that the bearing measured from digital compass is almost coincident with the expected azimuth bearing. The expected azimuth bearing at 0° is 144°; and 244° at an angle -90°, 54° at angle 90° on the protractor respectively. However, the measured azimuth bearing is increased as the digital compass turn to negative region; and decreased at the positive region. On a negative region, the bearing measured by compass is increasing about 10° from 143.98° at an angle 0° to 233.84° at angle -90°. And also, the bearing measured at positive region is decreasing about 10° from 143.98° to 53.9° at an angle 90°.

Refer to Appendix E, the root mean square error (RMSE) for each 10° interval is calculated. Taking the protractor angle at -80°, the RMSE value is calculated as below:

$$RMSE = \sqrt{\frac{1}{n}\sum_{j=1}^{n}\left(y_j - \hat{y}_j\right)^2}$$

$$RMSE = \sqrt{\frac{(225.46 - 224)^2 + (225.39 - 224)^2 + (223.65 - 224)^2}{3}}$$

$$RMSE = 1.1813°$$

From the calculation of RMSE, the RMSE value calculated is 1.1813°. This value is relatively higher compared with other RMSE at a different protractor angle. This is due to gross error and parallax error occurred while turning the digital compass on a protractor. However, the RMSE value obtained for protractor angle on -80° is acceptable since the error calculated is considered small. In summary, the digital compass can be integrated in the fan cleaning robot to examine the ability of robot in moving straight line.

4.2.4 Experiment Test 4: Angle decline of fan blade

Figure 4.8 is shown the graph of angle declined of the ceiling fan blade from its plane of rotation by comparing with two different weights of fan cleaning robot. Also, the data collected for this experiment are summarized in Appendix F.

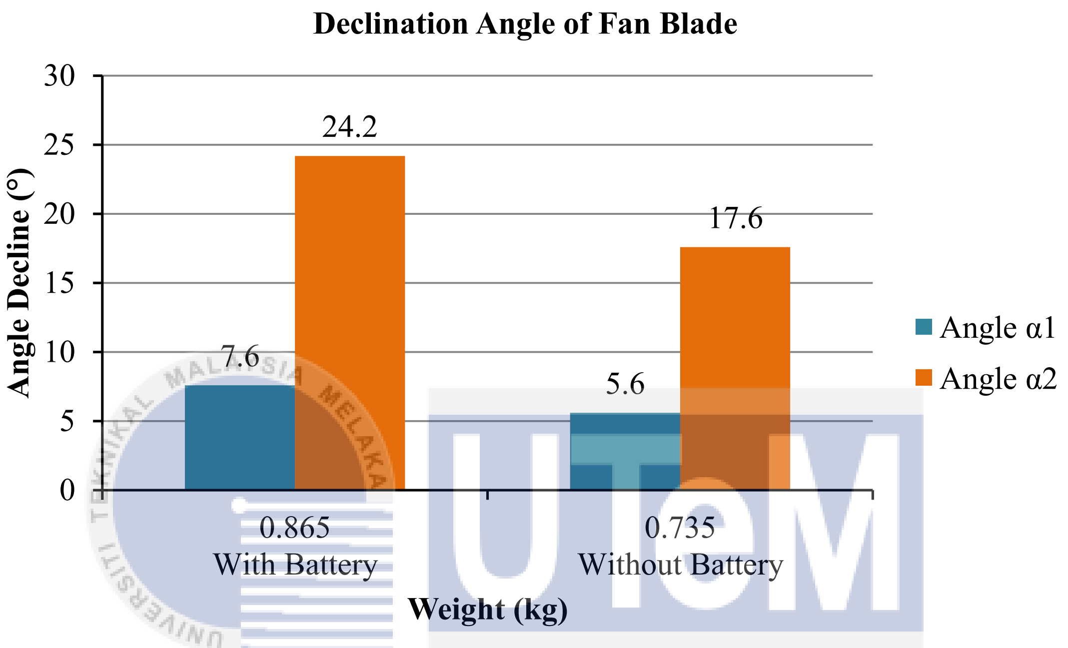

Figure 4.8: Graph of declination angle of fan blade about plane of rotation.

The graph in Figure 4.8 is shown the effect of fan cleaning robot weight on the fan blade. Two different weights are obtained and measured by using a digital weight scale machine, which is 0.865 kg for fan cleaning robot with 6V rechargeable battery as a power supply; and 0.735 kg without 6V rechargeable battery and replaced by 5V DC power adapter to supply power. From the results, fan cleaning robot with rechargeable battery pushed harder than robot without rechargeable battery due to it has a heavier weight. For the robot with battery, the average decline angle at angle α_1 is 7.6° downwards, and 24.2° at angle α_2. However, the decline angle is smaller for robot without the battery, which is 5.6° at angle α_1 and 17.6° at angle α_2. Meanwhile, the decline angle at angle α_1 and α_2 is taken based on the intercept point of tangent to the fan blade and the plane of rotation. After the robot is placed on fan blade, the blade is curved downwards; thus, the angles are taken in the tangential and the plane of rotation.

In addition, the standard deviation calculated for both value of weight at position angle α_1 and α_2 is considered small, which is 0.49 and 0.75 for a robot with rechargeable battery at angle α_1 and α_2 ; and 0.49 for both angle α_1 and α_2 for robot without rechargeable battery. Taking the measured angle at α_2 for a robot with rechargeable battery, the standard deviation is calculated.

$$\sigma = \sqrt{\frac{\sum_{i=1}^{n}(x_i - \bar{x})^2}{n}}$$

$$\sigma = \sqrt{\frac{(25-24.2)^2 + (25-24.2)^2 + (24-24.2)^2 + (23-24.2)^2 + (24-24.2)^2}{5}}$$

$$\sigma = 0.7483°$$

In summary, this experiment is important to determine the weight of fan cleaning robot in order to prevent the damage of the ceiling fan blade once the robot is placed on the blade. And also, the larger decline angle can affect the performance of robot locomotion on fan blade. If the fan blade has a larger decline angle to downwards, the robot is needed to decrease its total weight, and also implement the actuator with higher torque, so that the robot can move on fan blade.

4.2.5 Experiment Test 5: Velocity of fan cleaning robot

Figure 4.9 is shown a distance – time graph obtained from the results tabulated in Appendix G**.** This graph is comparing the type of power source to the effect of velocity and braking distance for fan cleaning robot.

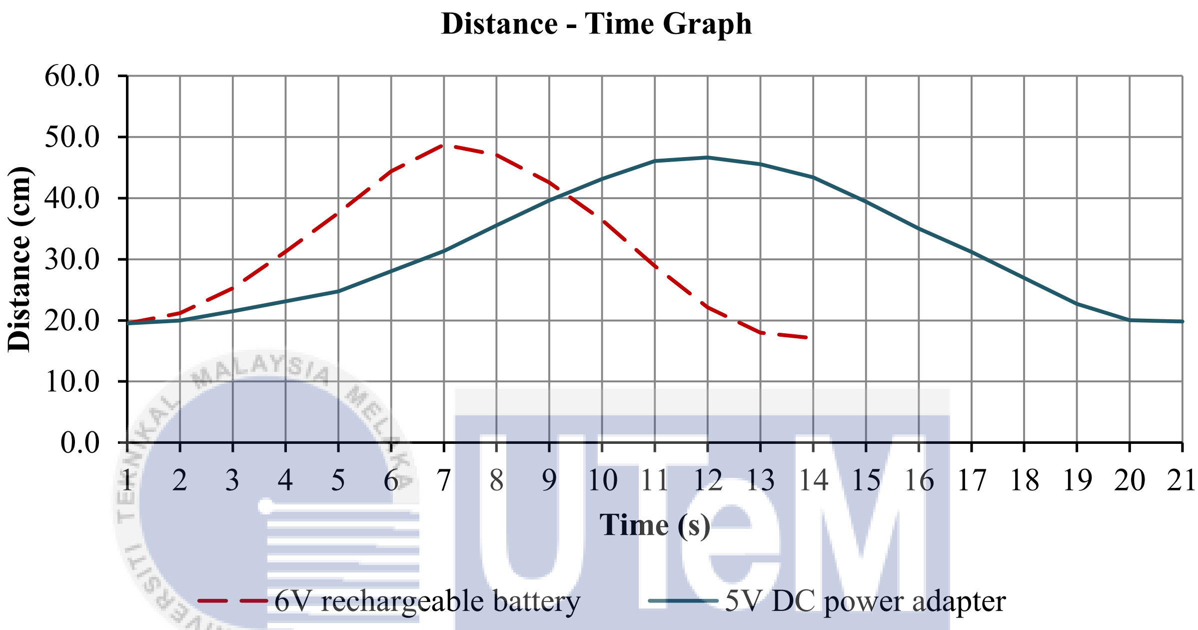

Figure 4.9: Distance – Time graph for fan cleaning robot.

Based on Figure 4.9, the diagram is shown a non-linear graph plotted for fan cleaning robot with two different power sources, which is 6V rechargeable battery and 5V DC power adapter. From the graph plotted, there is a significant result shown that the fan cleaning robot with battery can perform the cleaning task in 14 seconds, which is 7 seconds earlier compared to robot using a 5V DC power adapter, which is 21 seconds. This is due to the rechargeable battery provide higher voltage and current compare to 5V DC power adapter. Hence, higher speed is produced by battery compared to the power adapter. The gradient is shown the speed of fan cleaning robot, which is steeper for a robot with battery, hence higher velocity; and the gradient is gradual for robot using power adapter, so lower velocity.

Besides that, the graph also has shown the braking distance from the fan cleaning robot came to rest after the cleaning task is completed in 1 cycle. For robot using the power adapter as a power source, the braking distance is 20 cm, which is stopped at 0.5 cm before the starting position, 19.5 cm. However, the braking distance for a robot with battery overpasses the starting position, which is at 17.1 cm. This is due to the amount of inertia that fan cleaning robot possesses and the momentum produced is proportional to its mass. Therefore, the robot with battery is heavier and produced larger inertia and momentum, so the robot is overpassed the starting point. However, the robot is in risk fall down from fan blade if the inertia and momentum is too large.

In addition, the graph also has shown the fan cleaning robot to reach at the most inner part of the fan blade is different for using battery and power adapter as a power source respectively. From the graph, the robot with battery can reach at 48.8 cm, while the robot with power adapter only can reach at 46.7 cm in average. However, this does not mean that the robot with power adapter cannot reach at 49 cm position. Standard deviation is calculated for this situation, by taking the time at 12 second,

$$\sigma = \sqrt{\frac{\sum_{i=1}^{n}(x_i - \bar{x})^2}{n}}$$

$$\sigma = \sqrt{\frac{(49-46.7)^2 + (49-46.7)^2 + (47.8-46.7)^2 + (43-46.7)^2 + (44.5-46.7)^2}{5}}$$

$$\sigma = 2.4622\ cm$$

This is because the value of 46.7 cm is taking on average for 5 sample data, due to the time different to reach at that position. Also, gross error occurred due to human mistakes while placing the robot in the same position on fan blade when the experiment is carried out. Hence, the distance measured respect to the time taken is different.

4.2.6 Experiment Test 6: Angle deviated from straight line

Figure 4.10 is shown the graph of angle measured by a HMC5883L digital compass over time for fan cleaning robot to completely move on fan blade in the 1 cycle. The angle measured is in term of azimuth bearing to the North direction and the results are tabulated in Appendix H.

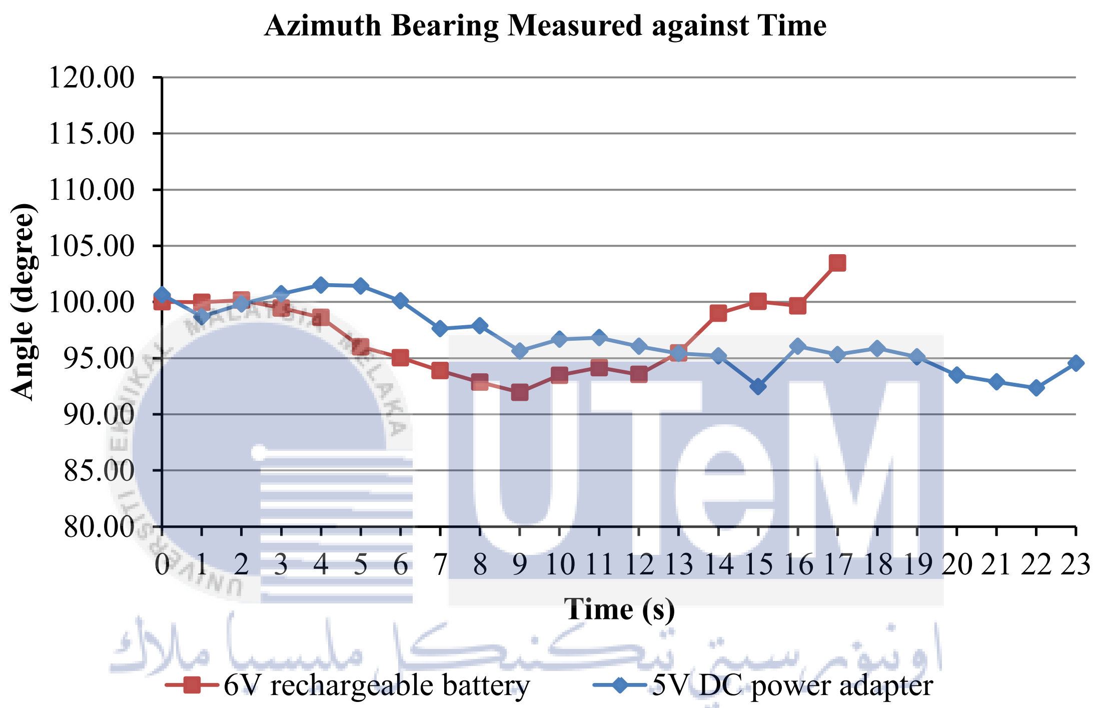

Figure 4.10: Azimuth bearing measured over time.

Based on Figure 4.10, the diagram is shown the swinging pattern of fan cleaning robot when moving in a straight line on the fan blade. The fan blade is located at 100° to the North direction in azimuth bearing, measured by a compass. Before the robot is turned on, the azimuth bearing from digital compass is compared with the reference angle to ensure the robot heading angle is the same.

From the figure above, the fan cleaning robot using battery as a power source has the maximum angle deviated of 8.04° in the right direction and 3.48° at left direction. However, for fan cleaning robot use power adapter as the power supply has a maximum angle deviated in the right direction, which is 7.53°; while the left direction is only 1.43°.

Hence, the graph is shown that the angle deviated from a straight line is higher for a robot with battery as power supply, compare with the robot using the power adapter. In addition, the graph also shown that at a time interval of 12 seconds, the movement of the robot is almost the same for a robot with battery and robot with power adapter respectively. Initially, the robot is deviated to left direction and then to right direction. However, the robot movement is changed at time interval of 13 seconds. The robot with battery is deviated to left direction again; while the robot with power adapter is continued to deviate at right direction of the fan blade.

Refer to Appendix H, the root mean square error (RMSE) of the angle deviated from a straight line is calculated every second when the robot is moving on fan blade. For the robot with battery as power supply, and taking the time at 10 seconds, the RMSE value is calculated as below:

$$RMSE = \sqrt{\frac{1}{n}\sum_{j=1}^{n}\left(y_j - \hat{y}_j\right)^2}$$

$$RMSE = \sqrt{\frac{(98.33-100)^2+(89.44-100)^2+(89.87-100)^2+(89.42-100)^2+(92.76-100)^2}{5}}$$

$$RMSE = 8.7324°$$

The RMSE value calculated above is 8.7324°. This value is shown that at a time interval of 10 seconds, the fan cleaning robot is deviated largely compare to the other RMSE value. However, the robot is still able to move in a straight line. This is due to the error occurred when the robot is moved on fan blade, such as systematic error and the instrumental error. However, the ceiling fan blade is designed to have an angle decline at the blade to increase the airflow efficiency. Hence at this time interval, the wheels of the robot cannot touch equally at both sides on fan blade. Thus, the robot is swing on fan blade and the pulley is guiding the robot to move so that both sides of the wheels can rotate on the fan blade again.

4.3 Equation of centre of mass for fan cleaning robot

Assuming Figure 4.11 is shown the free body diagram of a fan cleaning robot moving on an incline plane. Taking the weight of the robot without battery obtained in Experiment 4, the total weight is 0.735 kg. The front wheels of the robot carry 60% of the total weight and the rear part is 40%. Hence, the centre of mass of fan cleaning robot can be calculated. Figure 4.12 and Figure 4.13 is shown the location of the centre of mass on fan cleaning robot, display by purple colour in isometric view and side view respectively.

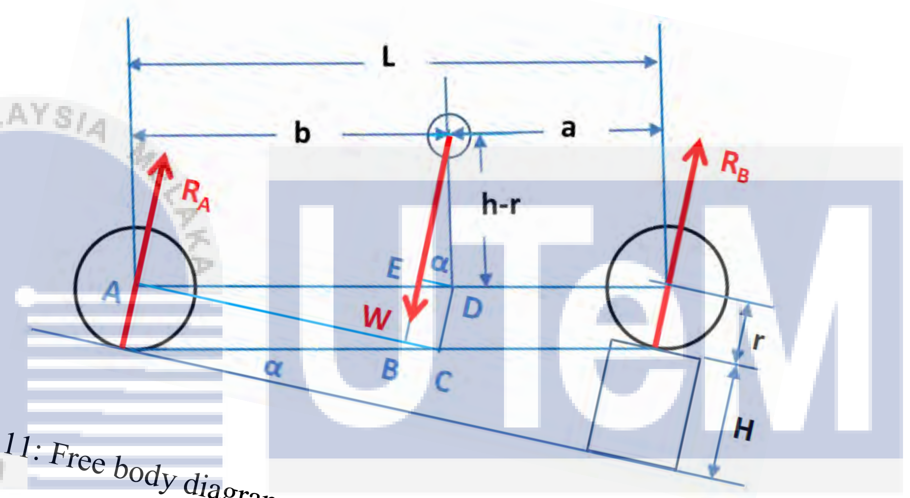

Figure 4.11: Free body diagram of fan cleaning robot on incline plane [13].

Given:

$L = 0.135$ cm $W = 0.735$ kg

$r = 0.018$ cm $R_A = 0.441$ kg

$\alpha = 17.6°$ $R_B = 0.294$ kg

From Equation 3.3,

$$R_A . L + W . b = 0$$

$$b = L\left(\frac{R_A}{W}\right)$$

$$b = 0.135\left(\frac{0.441}{0.735}\right) = 0.081\ m$$

$$\therefore \quad a = L - b$$

$$a = 0.135 - 0.081 = 0.054\ m$$

From Equation 3.6,

$$R_A.(L\cos\alpha) = W.[b\cos\alpha - (h-r)\sin\alpha]$$

$$h - r = \left[b - L\left(\frac{R_A}{W}\right)\right] cot\,\alpha$$

$$h = \left[b - L\left(\frac{R_A}{W}\right)\right] cot\,\alpha + r$$

$$h = \left[0.081 - 0.135\left(\frac{0.441}{0.735}\right)\right] cot\,17.6 + 1.8$$

$$h = 0.018\,m$$

Hence, the location of centre of mass for fan cleaning robot is:

$$\bar{x} = 0.081\,m \quad ; \quad \bar{y} = 0.018\,m$$

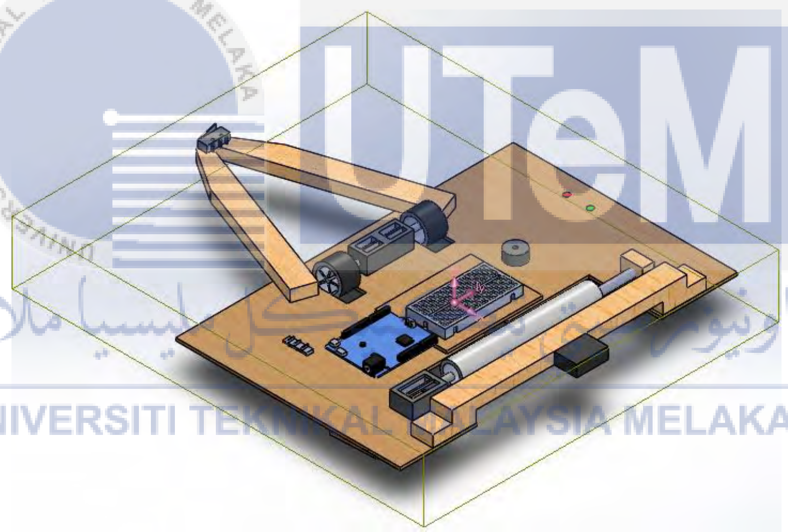

Figure 4.12: Isometric view of the centre of mass.

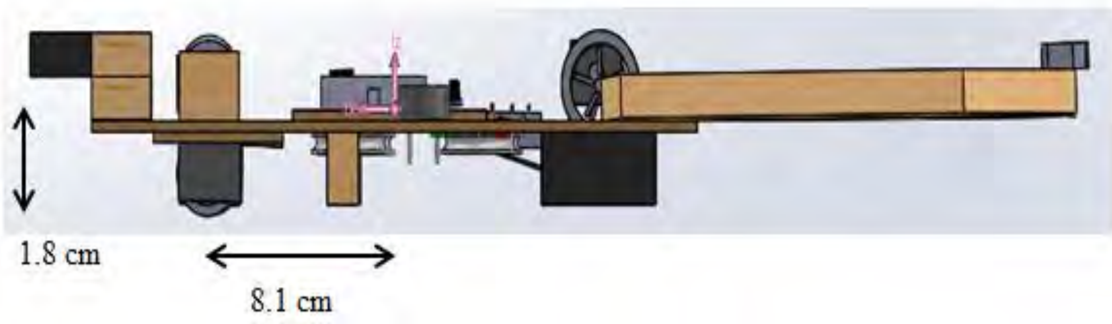

Figure 4.13: Side view of the centre of mass.

CHAPTER 5

CONCLUSION AND RECOMMENDATION

As a conclusion, this report introduced the development of ceiling fan cleaning robot. Through methodology, the fan cleaning robot is able to move in forward and reverse direction by triggering the sensors integrated in the system, without fall down from fan blade; and able to perform the cleaning task on ceiling fan blade. Meanwhile, plywood is used as the main material to construct the fan cleaning robot due to its characteristic of lightweight.

In addition, suitable components are selected and integrated in the system to actuate the fan cleaning robot. Since the fan blade in being pushed downwards after the robot is placed on fan blade, DC motors with gears has an advantage by providing higher torque to the robot move on fan blade, but the speed is slow. Infrared sensor and front limit switch are integrated in the system to actuate the DC motors. Also, LEDs and buzzer are used to indicate the start and stop operation of fan cleaning robot. All the process is controlled by microcontroller via the algorithms designed. Hence, the objective 1 has been achieved.

Besides that, a series of experiment is done to test the performance of fan cleaning robot in term of locomotion. The robot is tested by comparing the type of power supply, which is the 6V rechargeable battery and 5V DC power adapter. The overall results are shown using the power adapter as the power supply for fan cleaning robot is more suitable compare to a rechargeable battery. And also, the centre of mass of fan cleaning robot is determined from the weight obtained; the x-coordinate and y-coordinate is located at 8.1 cm and 1.8 cm respect to the origin. Thus, the objective 2 of this project has been achieved.

For this project, there are some recommendations for the future work:

1. The body structure of the robot can change to small and compact size. And also, lighter material is recommended to decrease the total weight of fan cleaning robot.
2. The actuator on fan cleaning robot is recommended to change its orientation from the horizontal shaft to a vertical shaft, so that it can move smoothly on fan blade, and will not swinging while moving.
3. Also, the mechanism used on pulley can replace by spring with high elasticity so that the fan cleaning robot can move on different size of the ceiling fan blade.
4. The ceiling fan cleaning robot can be further constructed by adding some additional features, such as a dustbin. A mini fan is located inside dustbin and function as a turbine to collect dust on fan blade.

REFERENCES

[1] W. Patent and T. Office, “A Technical Analysis of Autonomous Floor Cleaning Robots Based on US Granted Patents,” vol. 2, no. 7, 2013.

[2] “A robot in every home? -- ScienceDaily.” [Online]. Available: http://www.sciencedaily.com/releases/2004/10/041021085857.htm. [Accessed: 06-Nov-2014].

[3] E. Cleaners, “Cleaners and musculoskeletal disorders,” pp. 1–14.

[4] 古富文 and 何庆毫, “Ceiling fan cleaner,” C. N. Patent 203000878 U, 19-Jun-2013.

[5] 许福运 and 邵传兵, “Ceiling fan cleaner,” C. N. Patent 201019712 Y, 13-Feb-2008.

[6] S. Kim, “Autonomous Cleaning Robot : Rob oking System Integration and Overview,” no. April, pp. 4437–4441, 2004.

[7] “Robot Gossip: July 2005.” [Online]. Available: http://robotgossip.blogspot.com/2005_07_01_archive.html. [Accessed: 11-Nov-2014].

[8] J. Palacín, J. A. Salse, I. Valgañón, and X. Clua, “Building a Mobile Robot for a Floor-Cleaning Operation in Domestic Environments,” vol. 53, no. 5, pp. 1418–1424, 2004.

[9] T. Miyake, H. Ishihara, R. Shoji, and S. Yoshida, “Development of Small-Size Window Cleaning Robot A traveling direction control on Vertical surface Using accelerometer,” *2006 Int. Conf. Mechatronics Autom.*, pp. 1302–1307, Jun. 2006.

[10] J. Liu, H. Jiang, Z. Li, and H. Hu, “A Small Window-Cleaning Robot for Domestic Use,” *2009 Int. Conf. Artif. Intell. Comput. Intell.*, pp. 262–266, 2009.

[11] L. Yiwen, E. M. Joo, and O. L. Ping, “Design and Development of a Glass Cleaning Robot,” *2013 Fourth Int. Conf. Intell. Syst. Des. Eng. Appl.*, pp. 225–228, Nov. 2013.

[12] “Center of Mass.” [Online]. Available: http://oregonstate.edu/instruct/exss323/CM_Lab/Center of Mass.htm. [Accessed: 28-May-2015].

[13] “Finding the Car Center of Gravity/Mass (CG/CM).” [Online]. Available: http://www.thecartech.com/subjects/auto_eng/Center_of_Gravity.htm. [Accessed: 27-May-2015].

[14] “Arduino - ArduinoBoardLeonardo.” [Online]. Available: http://www.arduino.cc/en/Main/ArduinoBoardLeonardo. [Accessed: 29-May-2015].

[15] D. C. Mini-motors and B. Motors, “M31E-1 Series,” p. 31.

[16] E. Setup, “Tamiya „ Toy “ Motor Testing by Adam Borrell (a . k . a nexisnet),” pp. 1–12, 2013.

[17] “FC-130RA/SA.” [Online]. Available: http://www.mabuchi-motor.co.jp/cgi-bin/catalog/e_catalog.cgi?CAT_ID=fc_130rasa. [Accessed: 29-May-2015].

APPENDIX A

Gantt chart

Activity	Week																											
	FYP 1														FYP 2													
	1	2	3	4	5	6	7	8	9	10	11	12	13	14	1	2	3	4	5	6	7	8	9	10	11	12	13	14
Project Activities																												
Project Title Registration																												
Project Research																												
Preparation Proposal																												
Component Selection (Phase 1)																												
Algorithm Design																												
Study DC Motor																												
Study Arduino Microcontroller																												
Software Simulation																												
Hardware Development																												
Component Selection (Phase 2)																												
Integrate Hardware & Software																												
Performance Testing																												
Performance Analysis																												
Report Writing																												
Report Submission																												
FYP Presentation																												

APPENDIX B

Project Flowchart

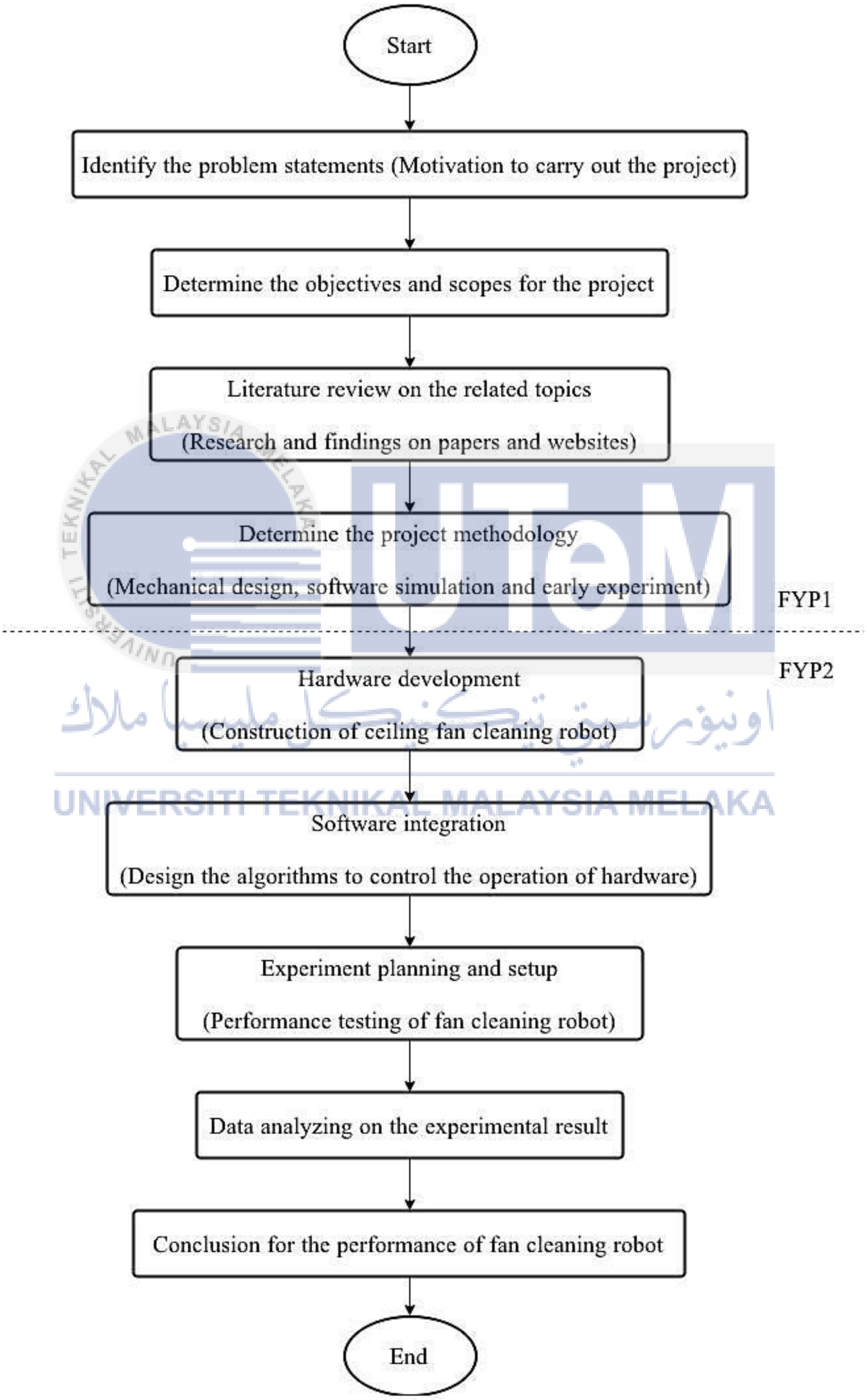

APPENDIX C

Result for Experiment Test 1: DC motor selection

1. Mitsumi M31E-1

Resistance, kΩ	Speed, RPM			Average Speed, RPM	Standard Deviation, RPM
	1	2	3		
0	1900	1880	1880	1887	9.4281
1	1488	1520	1504	1504	13.0639
2	1300	1300	1316	1305	7.5425
3	1136	1128	1116	1127	8.2192
4	950	940	950	947	4.7140
5	760	760	768	763	3.7712
6	384	384	384	384	0.0000
7	0	0	0	0	0.0000
8	0	0	0	0	0.0000
9	0	0	0	0	0.0000

2. FC-130SA-2270

Resistance, kΩ	Speed, RPM			Average Speed, RPM	Standard Deviation, RPM
	1	2	3		
0	17298	17865	18048	17737	319.2836
1	14476	14320	14668	14488	142.3236
2	10830	11160	11092	11027	142.2705
3	9120	9065	9080	9088	23.2140
4	8304	8276	8392	8324	49.4233
5	7708	7520	7520	7583	88.6240
6	5708	5708	5600	5672	50.9117
7	3760	3800	3800	3787	18.8562
8	0	0	0	0	0.0000
9	0	0	0	0	0.0000

3. Tamiya #70168 double gearbox

Resistance, kΩ	Speed, RPM			Average Speed, RPM	Standard Deviation, RPM
	1	2	3		
0	53	52	53	53	0.4714
1	46	46	46	46	0.0000
2	43	42	42	42	0.4714
3	39	38	38	38	0.4714
4	33	32	33	33	0.4714
5	29	28	28	28	0.4714
6	20	19	19	19	0.4714
7	7	7	7	7	0.0000
8	0	0	0	0	0.0000
9	0	0	0	0	0.0000

APPENDIX D

Result for Experiment Test 2: Distance measurement

Distance, cm	Output Voltage, V			Average Voltage, V	Standard Deviation, V
	1	2	3		
0	4.8	4.81	4.81	4.81	0.0047
2	4.72	4.72	4.71	4.72	0.0047
4	2.65	2.65	2.64	2.65	0.0047
6	1.4	1.4	1.41	1.40	0.0047
8	0.88	0.85	0.86	0.86	0.0125
10	0.59	0.56	0.57	0.57	0.0125
12	0.42	0.4	0.41	0.41	0.0082
14	0.32	0.31	0.31	0.31	0.0047
16	0.26	0.25	0.26	0.26	0.0047
18	0.22	0.21	0.22	0.22	0.0047
20	0.2	0.19	0.2	0.20	0.0047
22	0.18	0.18	0.18	0.18	0.0000
24	0.17	0.17	0.16	0.17	0.0047
26	0.16	0.16	0.16	0.16	0.0000
28	0.15	0.16	0.15	0.15	0.0047
30	0.15	0.15	0.15	0.15	0.0000

APPENDIX E

Result for Experiment Test 3: Accuracy test of digital compass

Protractor Angle, (°)	Expected Azimuth Bearing, (°)	Measured Azimuth Bearing, (°)			Average Azimuth Bearing, (°)	Error, (°)	Root Mean Square Error, RMSE (°)
		1	2	3			
-90	234	233.96	234.04	233.53	233.84	0.16	0.2733
-80	224	225.46	225.39	223.65	224.83	0.83	1.1813
-70	214	214.19	214.44	214.43	214.35	0.35	0.3718
-60	204	203.88	204.07	204	203.98	0.02	0.0802
-50	194	194.64	194.67	194.64	194.65	0.65	0.6502
-40	184	184.54	184.39	184.1	184.34	0.34	0.3889
-30	174	173.14	173.28	173	173.14	0.86	0.8676
-20	164	163.47	163.52	163.63	163.54	0.46	0.4648
-10	154	153.82	154.9	153.24	153.99	0.01	0.6880
0	144	144.01	144.05	143.89	143.98	0.02	0.0700
10	134	133.69	134.22	134.82	134.24	0.24	0.5218
20	124	123.19	123.68	123.8	123.56	0.44	0.5159
30	114	114.63	114.2	113.77	114.20	0.20	0.4041
40	104	103.3	104.34	104.9	104.18	0.18	0.6869
50	94	93.84	92.83	94.34	93.67	0.33	0.7095
60	84	84.54	84.16	83.82	84.17	0.17	0.3414
70	74	72.61	73.95	73.95	73.50	0.50	0.8036
80	64	64.19	62.47	64.68	63.78	0.22	0.9729
90	54	53.65	53.67	54.37	53.90	0.10	0.3504

APPENDIX F

Result for Experiment Test 4: Angle decline of fan blade

1. Fan cleaning robot with battery: 0.865 kg

		Declination Angle, (°)	
		Angle α_1	Angle α_2
Sample	1	8	25
	2	8	25
	3	7	24
	4	7	23
	5	8	24

Average Angle Decline, (°)	7.6	24.2
Standard Deviation, (°)	0.4899	0.7483

2. Fan cleaning robot without battery: 0.735 kg

		Declination Angle, (°)	
		Angle α_1	Angle α_2
Sample	1	5	18
	2	5	18
	3	6	17
	4	6	18
	5	6	17

Average Angle Decline, (°)	5.6	17.6
Standard Deviation, (°)	0.4899	0.4899

APPENDIX G

Result for Experiment Test 5: Velocity of fan cleaning robot

1. Fan cleaning robot with battery: 0.865 kg

Time, s	Distance, cm					Average Distance, cm	Standard Deviation, cm
	1	2	3	4	5		
1	19.5	19.5	19.5	19.5	19.5	19.5	0.0000
2	20	20	20	20	20	20.0	0.0000
3	20.5	21	21	24	21	21.5	1.2649
4	21.9	22.5	22.8	26.4	22	23.1	1.6726
5	24	24.8	25	27	23	24.8	1.3230
6	26.6	27	28	33.5	25	28.0	2.9054
7	30	31	32	37.7	26	31.3	3.7766
8	33	35.4	37	43.4	29	35.6	4.7571
9	37.7	39.5	41.4	47.5	32	39.6	5.0404
10	40.8	43.9	46	49	36	43.1	4.4621
11	45	47.9	48.8	47.6	41	46.1	2.8281
12	49	49	47.8	43	44.5	46.7	2.4622
13	48	47.4	46	38	48.4	45.6	3.8666
14	46	44	42	36	49	43.4	4.3635
15	42	40	38	30	47	39.4	5.5714
16	38	35.8	33.5	25.7	42	35.0	5.4292
17	34	31.5	30	22.5	38	31.2	5.1245
18	29	27	25	18.3	35.4	26.9	5.5540
19	24	23	22	17.9	26.5	22.7	2.8195
20	21	22	18.3	17.9	21	20.0	1.6305
21	20.4	22	18.3	17.9	20.4	19.8	1.5113

2. Fan cleaning robot without battery: 0.735 kg

Time, s	Distance, cm					Average Distance, cm	Standard Deviation, cm
	1	2	3	4	5		
1	19.5	19.5	19.5	19.5	19.5	19.5	0.0000
2	21	21	21.5	21.5	21	21.2	0.2449
3	25.5	26	25	25.8	24	25.3	0.7144
4	33	32.5	30.8	32	28	31.3	1.7862
5	39	39	37	38	35	37.6	1.4967
6	44	46	44	45	43	44.4	1.0198
7	49	49	48.8	49	48	48.8	0.3878
8	45.4	47	49	45	49	47.1	1.7046
9	41	42	45	40	44.8	42.6	2.0136
10	33.5	34.7	40	34	40	36.4	2.9316
11	25	29	32	26.5	32	28.9	2.8355
12	19.5	21	25	20	25	22.1	2.4166
13	17.9	16.5	19.5	17	19	18.0	1.1409
14	17.9	16.5	17	17	17	17.1	0.4534

APPENDIX H

Result for Experiment Test 6: Angle deviated from straight line

1. **Fan cleaning robot with battery: 0.865 kg**

Time, s	Measured Azimuth Bearing, (°)					Average Azimuth Bearing, (°)	Error, (°)	Root Mean Square Error, RMSE (°)
	1	2	3	4	5			
1	102.67	100.47	98.7	99.09	99.17	100.02	0.02	1.4531
2	101.68	101.68	98	99.51	99.02	99.98	0.02	1.4728
3	103.68	99.14	99.58	99.09	99.31	100.16	0.16	1.7755
4	101.94	99.02	98.76	97.48	100.13	99.47	0.53	1.5893
5	101.44	95.66	98.36	96.68	100.95	98.62	1.38	2.6655
6	99.44	89.54	97.76	93.72	99.58	96.01	3.99	5.5562
7	98.39	89.86	98.41	89.84	98.69	95.04	4.96	6.5251
8	96.32	90.28	94.83	90.81	97.18	93.88	6.12	6.7403
9	98.15	92.02	89.34	90.86	93.97	92.87	7.13	7.7542
10	98.33	89.44	89.87	89.42	92.76	91.96	8.04	8.7324
11	97.71	93.36	90.79	94.54	90.96	93.47	6.53	7.0099
12	98.39	94.85	89.4	95.5	92.65	94.16	5.84	6.5688
13	98.24	95.13	90.05	95.19	89.12	93.55	6.45	7.3120
14	96.1	94.86	95.06	94.47	96.85	95.47	4.53	4.6160
15	95.03	103.04	95.7	105.17	96.02	98.99	1.01	4.3589
16	105.03	103.67	95.06	101.36	95.11	100.05	0.05	4.2175
17	104.89	102.88	94.76	101.55	94.22	99.66	0.34	4.3698
18	105.12	103.14	104.55	100.56	104.01	103.48	3.48	3.8254

2. Fan cleaning robot without battery: 0.735 kg

Time, s	Measured Azimuth Bearing, (°)					Average Azimuth Bearing, (°)	Error, (°)	Root Mean Square Error, RMSE (°)
	1	2	3	4	5			
0	98.89	98.24	101.11	98.67	106.41	100.66	0.664	3.1119
1	100.01	91.04	100.06	97.93	104.42	98.69	1.308	4.5630
2	106.67	87.85	101.68	99.02	103.86	99.82	0.184	6.4930
3	102.72	85.16	106.67	105.76	103.37	100.74	0.736	7.9580
4	102.18	87.05	107.83	105.94	104.57	101.51	1.514	7.6149
5	103.12	87.83	107.28	105.76	103.17	101.43	1.432	7.1284
6	102.53	87.64	104.31	107.09	98.97	100.11	0.108	6.7687
7	99.78	86.16	101.64	103.44	97.09	97.62	2.378	6.5511
8	101.04	87.45	101.46	102.48	97	97.89	2.114	5.9307
9	99.78	80.73	102.36	98.71	96.66	95.65	4.352	8.8292
10	102.81	87.41	99.74	94.85	98.58	96.68	3.322	6.2452
11	100.72	92.41	100.46	95.33	95.24	96.83	3.168	4.5344
12	98.86	95.9	99.71	94.86	90.97	96.06	3.94	5.0230
13	98.18	94.65	99.02	92.59	92.73	95.43	4.566	5.3039
14	96.96	92.74	99.51	93.34	93.52	95.21	4.786	5.4504
15	96.86	92.44	93.57	80.3	99.18	92.47	7.53	9.9712
16	96.42	94.14	99.21	91.07	99.4	96.05	3.952	5.0574
17	95.24	91.87	95.52	96.32	97.68	95.33	4.674	5.0547
18	95.14	93.11	96.98	95.53	98.6	95.87	4.128	4.5200
19	92.36	93.2	98.02	96.23	95.79	95.12	4.88	5.3003
20	90.98	92.89	95.49	94.26	93.81	93.49	6.514	6.6860
21	91.2	93.12	92.83	92.41	94.91	92.89	7.106	7.2069
22	90.78	93.23	93.32	93.45	90.95	92.35	7.654	7.7494
23	90.88	93.25	98.88	98.39	91.3	94.54	5.46	6.4540

APPENDIX I

Design of Ceiling Fan Cleaning Robot in SolidWorks

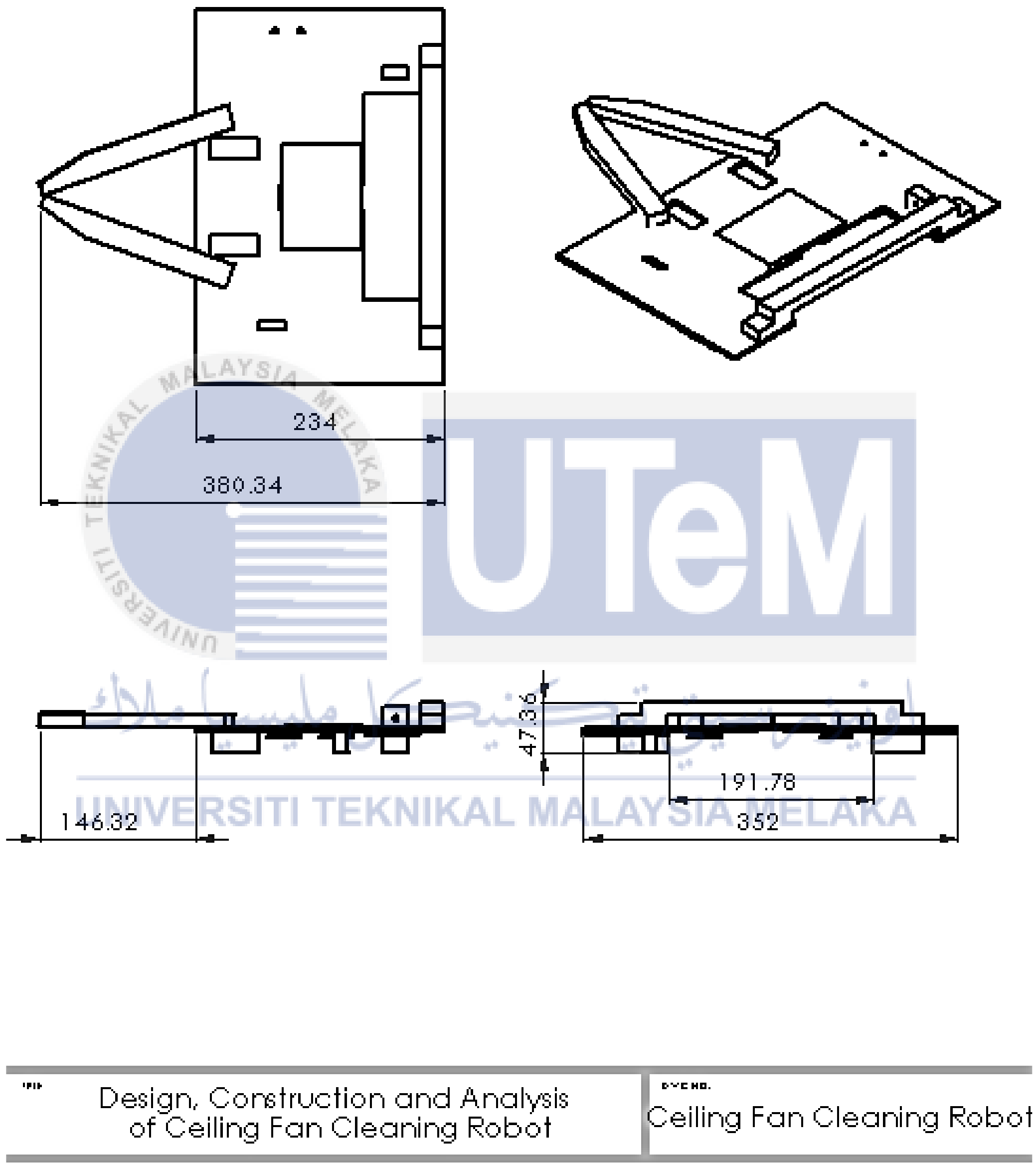

APPENDIX J

Design of Extension Rod in SolidWorks

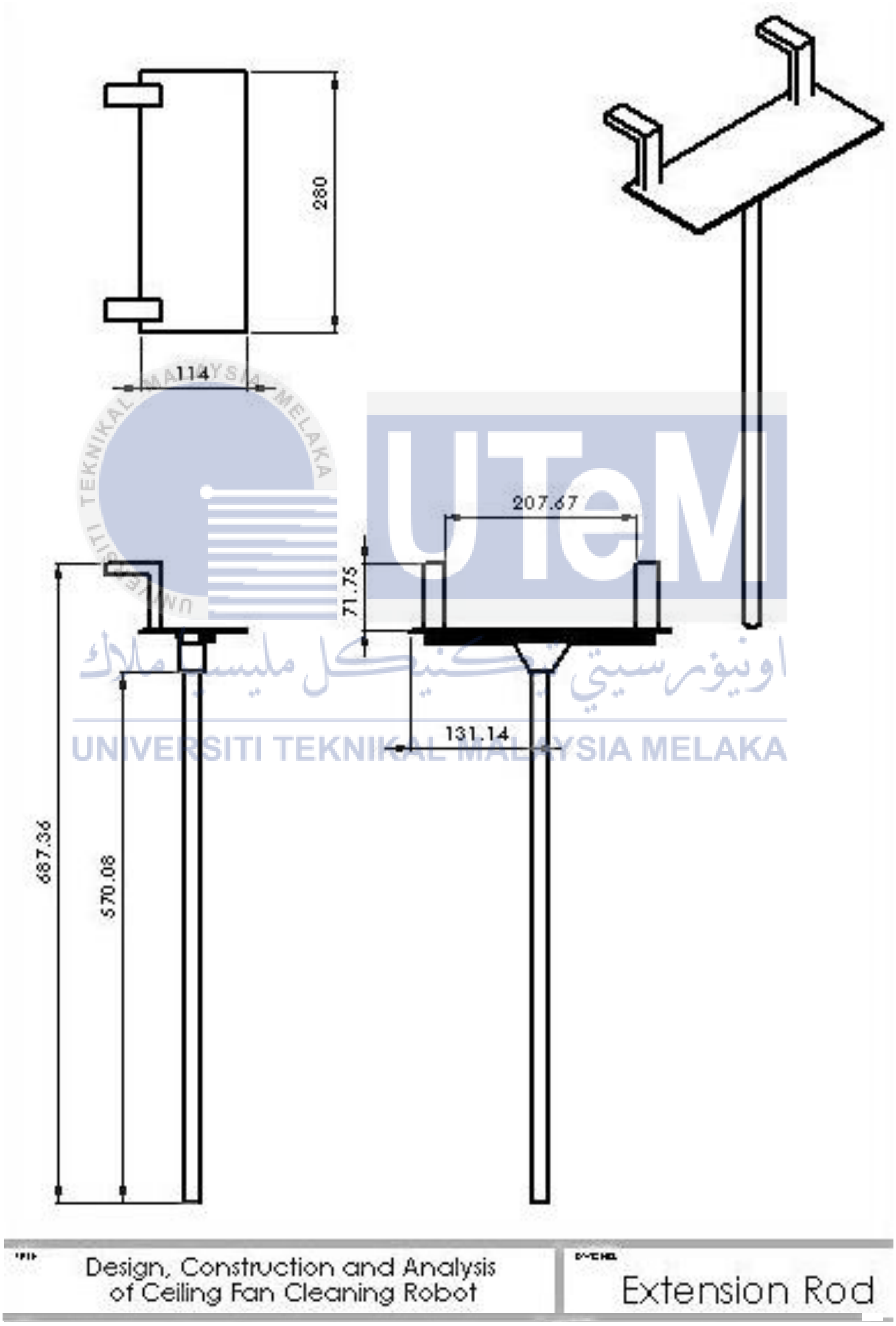

APPENDIX K

Complete Arduino Program for Ceiling Fan Cleaning Robot

```
#include <Wire.h>
#include <HMC5883L.h>

// Pin declaration
HMC5883L compass;
int error = 0;
int MA1 = 9;
int MA2 = 10;
int MA3 = 11;
int MA4 = 12;
int onoff = 6;
int button = 5;
int irpin = 4;
int redled = A5;
int greenled = A4;
int pushcount = 0;
int pushstate = 1;
int lastpushstate = 0;

void setup()                    // Setting the port number
{
  Serial.begin(9600);
  pinMode(MA1, OUTPUT);
  pinMode(MA2, OUTPUT);
  pinMode(MA3, OUTPUT);
  pinMode(MA4, OUTPUT);
  pinMode(redled, OUTPUT);
  pinMode(greenled, OUTPUT);
  pinMode(onoff, INPUT);
```

```
  pinMode(irpin, INPUT);
  pinMode(button, INPUT);

  Serial.println("Starting the I2C interface.");
  Wire.begin();
  Serial.println("Constructing new HMC5883L");
  compass = HMC5883L();
  Serial.println("Setting scale to +/- 1.3 Ga");
  error = compass.SetScale(1.3);
  if(error != 0)
    Serial.println(compass.GetErrorText(error));
  Serial.println("Setting measurement mode to continous.");
  error = compass.SetMeasurementMode(Measurement_Continuous);
  if(error != 0)
    Serial.println(compass.GetErrorText(error));
}

void loop()
{
  angle();
  int ir = digitalRead(irpin);
  int pin = digitalRead(button);

  if(digitalRead(onoff)==0)             // Turn on the robot
  {
    if((ir>0)&&(pin<1))                 // If infrared not triggered
    {
      analogWrite(greenled, 255);
      forward();                        // Robot move in forward direction
    }
    else if((ir<1)&&(pin>0))            // If infrared and front limit switch triggered
    {
      analogWrite(greenled, 255);
      reverse();                        // Robot move in reverse direction
```

```
    }
  }
  else if(digitalRead(onoff)==1)        // Turn off the robot and reset the routine
  {
    halt();
    blinkled();
    pushcount = 0;
    pushstate = 1;
    lastpushstate = 0;
  }
  stoploop();
}

void forward()                          // Robot move forward
{
  digitalWrite(MA2, LOW);
  digitalWrite(MA1, 255);
  digitalWrite(MA4, LOW);
  digitalWrite(MA3, 255);
}

void reverse()                          // Robot move reverse
{
  digitalWrite(MA1, LOW);
  digitalWrite(MA2, 255);
  digitalWrite(MA3, LOW);
  digitalWrite(MA4, 255);
}

void halt()                             // Robot stop
{
  digitalWrite(MA1, LOW);
  digitalWrite(MA2, LOW);
  digitalWrite(MA3, LOW);
```

```
  digitalWrite(MA4, LOW);
}

void blinkled()                              // Red LED and buzzer turn on
{
  analogWrite(greenled, 0);

  for (int i=0; i<3; i++)
  {
    analogWrite(redled, 255);
    delay(400);
    analogWrite(redled, 0);
    delay(400);
  }
}

void stoploop()                              // Counter to halt the program
{
  pushstate = digitalRead(irpin);
  if(pushstate != lastpushstate)
  {
    if(pushstate==1)
    {
      analogWrite(greenled, 0);
      pushcount++;
    }
  }
  lastpushstate = pushstate;

  if(pushcount%3==0)                         // Set the number to counter
  {
    halt();
    blinkled();
  }
```

```
}
void angle()                              // Read the heading direction of digital compass
{
  MagnetometerRaw raw = compass.ReadRawAxis();
  MagnetometerScaled scaled = compass.ReadScaledAxis();

  int MilliGauss_OnThe_XAxis = scaled.XAxis;
  float heading = atan2(scaled.YAxis, scaled.XAxis);
  float declinationAngle = 0.0008727;
  heading += declinationAngle;

  if(heading < 0)
    heading += 2*PI;

  if(heading > 2*PI)
    heading -= 2*PI;

  float headingDegrees = heading * 180/M_PI;
  Output(raw, scaled, heading, headingDegrees);
  delay(1000);
}

void Output(MagnetometerRaw raw, MagnetometerScaled scaled, float heading, float
headingDegrees)                           // Display the azimuth angle in serial monitor
{
  Serial.print("Raw:\t");
  Serial.print(raw.XAxis);
  Serial.print("  ");
  Serial.print(raw.YAxis);
  Serial.print("  ");
  Serial.print(raw.ZAxis);
  Serial.print("  \tScaled:\t");
```

```
  Serial.print(scaled.XAxis);
  Serial.print("  ");
  Serial.print(scaled.YAxis);
  Serial.print("  ");
  Serial.print(scaled.ZAxis);

  Serial.print("  \tHeading:\t");
  Serial.print(heading);
  Serial.print(" Radians  \t");
  Serial.print(headingDegrees);
  Serial.println(" Degrees  \t");
}
```

APPENDIX K

Manual for Ceiling Fan Cleaning Robot

1. Program design

i. To change the port number of DC motors on microcontroller, refer to *MA1* to *MA4* at *void setup*.

ii. To change the number of loop for cleaning, change *if (pushcount %* ***number****==0)*. The ***number*** value may bigger than *1*.

iii. The speed of DC motor rotate can be changed at *digitalWrite(****port****,* ***value****)* in user declaration functions *void forward* and *void reverse*. The ***port*** is refer to the port number of DC motor to microcontroller, ***value*** is the speed to set on DC motor.

2. Fan cleaning robot manual control

i. Powered the Arduino microcontroller via the USB connection; and the L293D H-Bridge with an external power supply in the range of 5V to 9V.

ii. Place the fan cleaning robot on fan blade by using extension rod.

iii. The infrared sensor does not detect the fan blade, so the robot will be moved forward; and front limit switch trigger the robot move in reverse direction.

iv. The process is repeated by setting the numbers of looping.

v. Switch off the power supply and remove the cable when the fan cleaning robot is not in used.